bursting activity even in the islet preparations. However, it should be noted that in other islet studies, thapsigargin induced a sustained increase in $[Ca^{2+}]_i$ (Worley et al., 1994b; Gilon et al., 1999; Kanno et al., 2002), accompanied by a continuous firing of action potentials (Worley et al., 1994b). Furthermore, both of these responses have been observed in the same experimental study (Miura et al., 1997). At present, it might be speculated that our cell model represents only a given population of β cells, or that the cell-to-cell electrical coupling among different populations of cell types within the islet can produce different patterns in the thapsigargin response.

Although the current system was much improved compared with the previous β-cell models by adding individual current components in the molecular level, further refinement of the formulation will be necessary according to new experimental data in future, especially in respect to temperature effects on channel kinetics. Furthermore, compared with the electrophysiological formulations, the description of energy metabolism is quite simplified in our β-cell model. Therefore, it is beyond the scope of this study to reproduce an ultraslow bursting rhythm with periods >5 min, which have been suspected to be of metabolic origin (Henquin et al., 1982; Bertram et al., 2004). Moreover, the effect of $[Ca^{2+}]_i$ on ATP production was not considered in our model. Keizer and Magnus (1989) assumed that Ca^{2+} entry into the mitochondria depolarized the matrix membrane to inhibit ATP production. However, the opposite effect has also been proposed, namely that an increase in $[Ca^{2+}]_i$ might facilitate ATP production by activating dehydrogenases within the TCA cycle (Cortassa et al., 2003). The net effect of $[Ca^{2+}]_i$ on ATP production is not quantitatively known at present. Therefore, it will be important to include more precise models for glycolysis (Smolen, 1995; Bertram et al., 2004), TCA cycle, and oxidative phosphorylation (Dzbek and Korzeniewski, 2008) in future formulations.

We thank Professor T. Powell for fruitful discussion and for improving the English of this paper.

This work was supported by the Biomedical Cluster Kansai project; a Grant-in-Aid (22590216 to C.Y. Cha and 22390039 to A. Noma) from the Ministry of Education, Culture, Sports, Science and Technology of Japan; and the Ritsumeikan-Global Innovation Research Organization at Ritsumeikan University.

Lawrence G. Palmer served as editor.

Submitted: 7 February 2011
Accepted: 7 June 2011

REFERENCES

Ämmälä, C., P.O. Berggren, K. Bokvist, and P. Rorsman. 1992. Inhibition of L-type calcium channels by internal GTP [gamma S] in mouse pancreatic beta cells. *Pflugers Arch.* 420:72–77. doi:10.1007/BF00378643

Antunes, C.M., A.P. Salgado, L.M. Rosário, and R.M. Santos. 2000. Differential patterns of glucose-induced electrical activity and intracellular calcium responses in single mouse and rat pancreatic islets. *Diabetes.* 49:2028–2038. doi:10.2337/diabetes.49.12.2028

Arkhammar, P., L. Juntti-Berggren, O. Larsson, M. Welsh, E. Nånberg, A. Sjöholm, M. Köhler, and P.O. Berggren. 1994. Protein kinase C modulates the insulin secretory process by maintaining a proper function of the beta-cell voltage-activated Ca^{2+} channels. *J. Biol. Chem.* 269:2743–2749.

Ashcroft, F.M., and M. Kakei. 1989. ATP-sensitive K^+ channels in rat pancreatic beta-cells: modulation by ATP and Mg^{2+} ions. *J. Physiol.* 416:349–367.

Ashcroft, F.M., and P. Rorsman. 1989. Electrophysiology of the pancreatic beta-cell. *Prog. Biophys. Mol. Biol.* 54:87–143. doi:10.1016/0079-6107(89)90013-8

Ashcroft, F.M., D.E. Harrison, and S.J. Ashcroft. 1984. Glucose induces closure of single potassium channels in isolated rat pancreatic beta-cells. *Nature.* 312:446–448. doi:10.1038/312446a0

Atwater, I., B. Ribalet, and E. Rojas. 1979. Mouse pancreatic beta-cells: tetraethylammonium blockage of the potassium permeability increase induced by depolarization. *J. Physiol.* 288:561–574.

Bertram, R., and A. Sherman. 2004. A calcium-based phantom bursting model for pancreatic islets. *Bull. Math. Biol.* 66:1313–1344. doi:10.1016/j.bulm.2003.12.005

Bertram, R., M.J. Butte, T. Kiemel, and A. Sherman. 1995a. Topological and phenomenological classification of bursting oscillations. *Bull. Math. Biol.* 57:413–439.

Bertram, R., P. Smolen, A. Sherman, D. Mears, I. Atwater, F. Martin, and B. Soria. 1995b. A role for calcium release-activated current (CRAC) in cholinergic modulation of electrical activity in pancreatic beta-cells. *Biophys. J.* 68:2323–2332. doi:10.1016/S0006-3495(95)80414-5

Bertram, R., J. Previte, A. Sherman, T.A. Kinard, and L.S. Satin. 2000. The phantom burster model for pancreatic beta-cells. *Biophys. J.* 79:2880–2892. doi:10.1016/S0006-3495(00)76525-8

Bertram, R., L. Satin, M. Zhang, P. Smolen, and A. Sherman. 2004. Calcium and glycolysis mediate multiple bursting modes in pancreatic islets. *Biophys. J.* 87:3074–3087. doi:10.1529/biophysj.104.049262

Bokvist, K., C. Ämmälä, P.O. Berggren, P. Rorsman, and K. Wåhlander. 1991. Alpha 2-adrenoreceptor stimulation does not inhibit L-type calcium channels in mouse pancreatic beta-cells. *Biosci. Rep.* 11:147–157. doi:10.1007/BF01182483

Bozem, M., and J.C. Henquin. 1988. Glucose modulation of spike activity independently from changes in slow waves of membrane potential in mouse B-cells. *Pflugers Arch.* 413:147–152. doi:10.1007/BF00582524

Braun, M., R. Ramracheya, M. Bengtsson, Q. Zhang, J. Karanauskaite, C. Partridge, P.R. Johnson, and P. Rorsman. 2008. Voltage-gated ion channels in human pancreatic beta-cells: electrophysiological characterization and role in insulin secretion. *Diabetes.* 57:1618–1628. doi:10.2337/db07-0991

Brini, M., and E. Carafoli. 2009. Calcium pumps in health and disease. *Physiol. Rev.* 89:1341–1378. doi:10.1152/physrev.00032.2008

Caride, A.J., A.R. Penheiter, A.G. Filoteo, Z. Bajzer, A. Enyedi, and J.T. Penniston. 2001. The plasma membrane calcium pump displays memory of past calcium spikes. Differences between isoforms 2b and 4b. *J. Biol. Chem.* 276:39797–39804. doi:10.1074/jbc.M104380200

Cha, C.Y., Y. Himeno, T. Shimayoshi, A. Amano, and A. Noma. 2009. A novel method to quantify contribution of channels and transporters to membrane potential dynamics. *Biophys. J.* 97:3086–3094. doi:10.1016/j.bpj.2009.08.060

Cha, C.Y., E. Santos, A. Amano, T. Shimayoshi, and A. Noma. 2011. Time-dependent changes in membrane excitability during glucose-induced bursting activity in pancreatic β cells. *J. Gen. Physiol.* 138:39–47.

Chapman, J.B., E.A. Johnson, and J.M. Kootsey. 1983. Electrical and biochemical properties of an enzyme model of the sodium pump. *J. Membr. Biol.* 74:139–153. doi:10.1007/BF01870503

Chay, T.R. 1996. Electrical bursting and luminal calcium oscillation in excitable cell models. *Biol. Cybern.* 75:419–431. doi:10.1007/s004220050307

Chay, T.R. 1997. Effects of extracellular calcium on electrical bursting and intracellular and luminal calcium oscillations in insulin secreting pancreatic beta-cells. *Biophys. J.* 73:1673–1688. doi:10.1016/S0006-3495(97)78199-2

Chay, T.R., and J. Keizer. 1983. Minimal model for membrane oscillations in the pancreatic beta-cell. *Biophys. J.* 42:181–190. doi:10.1016/S0006-3495(83)84384-7

Cheng, H., A. Beck, P. Launay, S.A. Gross, A.J. Stokes, J.P. Kinet, A. Fleig, and R. Penner. 2007. TRPM4 controls insulin secretion in pancreatic beta-cells. *Cell Calcium.* 41:51–61. doi:10.1016/j.ceca.2006.04.032

Chow, R.H., P.E. Lund, S. Löser, U. Panten, and E. Gylfe. 1995. Coincidence of early glucose-induced depolarization with lowering of cytoplasmic Ca^{2+} in mouse pancreatic beta-cells. *J. Physiol.* 485:607–617.

Colsoul, B., A. Schraenen, K. Lemaire, R. Quintens, L. Van Lommel, A. Segal, G. Owsianik, K. Talavera, T. Voets, R.F. Margolskee, et al. 2010. Loss of high-frequency glucose-induced Ca^{2+} oscillations in pancreatic islets correlates with impaired glucose tolerance in Trpm5-/- mice. *Proc. Natl. Acad. Sci. USA.* 107:5208–5213. doi:10.1073/pnas.0913107107

Cook, D.L., and C.N. Hales. 1984. Intracellular ATP directly blocks K^+ channels in pancreatic B-cells. *Nature.* 311:271–273. doi:10.1038/311271a0

Cortassa, S., M.A. Aon, E. Marbán, R.L. Winslow, and B. O'Rourke. 2003. An integrated model of cardiac mitochondrial energy metabolism and calcium dynamics. *Biophys. J.* 84:2734–2755. doi:10.1016/S0006-3495(03)75079-6

Dean, P.M., E.K. Matthews, and Y. Sakamoto. 1975. Pancreatic islet cells: effects of monosaccharides, glycolytic intermediates and metabolic inhibitors on membrane potential and electrical activity. *J. Physiol.* 246:459–478.

Diederichs, F. 2006. Mathematical simulation of membrane processes and metabolic fluxes of the pancreatic beta-cell. *Bull. Math. Biol.* 68:1779–1818. doi:10.1007/s11538-005-9053-9

Düfer, M., B. Gier, D. Wolpers, P. Krippeit-Drews, P. Ruth, and G. Drews. 2009. Enhanced glucose tolerance by SK4 channel inhibition in pancreatic beta-cells. *Diabetes.* 58:1835–1843. doi:10.2337/db08-1324

Dunne, M.J., and O.H. Petersen. 1986. Intracellular ADP activates K^+ channels that are inhibited by ATP in an insulin-secreting cell line. *FEBS Lett.* 208:59–62. doi:10.1016/0014-5793(86)81532-0

Dzbek, J., and B. Korzeniewski. 2008. Control over the contribution of the mitochondrial membrane potential (DeltaPsi) and proton gradient (DeltapH) to the protonmotive force (Deltap). In silico studies. *J. Biol. Chem.* 283:33232–33239. doi:10.1074/jbc.M802404200

Elwess, N.L., A.G. Filoteo, A. Enyedi, and J.T. Penniston. 1997. Plasma membrane Ca^{2+} pump isoforms 2a and 2b are unusually responsive to calmodulin and Ca^{2+}. *J. Biol. Chem.* 272:17981–17986. doi:10.1074/jbc.272.29.17981

Enyedi, A., A.G. Filoteo, G. Gardos, and J.T. Penniston. 1991. Calmodulin-binding domains from isozymes of the plasma membrane Ca^{2+} pump have different regulatory properties. *J. Biol. Chem.* 266:8952–8956.

Fridlyand, L.E., N. Tamarina, and L.H. Philipson. 2003. Modeling of Ca^{2+} flux in pancreatic beta-cells: role of the plasma membrane and intracellular stores. *Am. J. Physiol. Endocrinol. Metab.* 285:E138–E154.

Fridlyand, L.E., L. Ma, and L.H. Philipson. 2005. Adenine nucleotide regulation in pancreatic beta-cells: modeling of ATP/ADP-Ca^{2+} interactions. *Am. J. Physiol. Endocrinol. Metab.* 289:E839–E848. doi:10.1152/ajpendo.00595.2004

Fridlyand, L.E., D.A. Jacobson, A. Kuznetsov, and L.H. Philipson. 2009. A model of action potentials and fast Ca^{2+} dynamics in pancreatic beta-cells. *Biophys. J.* 96:3126–3139. doi:10.1016/j.bpj.2009.01.029

Fridlyand, L.E., N. Tamarina, and L.H. Philipson. 2010. Bursting and calcium oscillations in pancreatic beta-cells: specific pacemakers for specific mechanisms. *Am. J. Physiol. Endocrinol. Metab.* 299:E517–E532. doi:10.1152/ajpendo.00177.2010

Gall, D., J. Gromada, I. Susa, P. Rorsman, A. Herchuelz, and K. Bokvist. 1999. Significance of Na/Ca exchange for Ca^{2+} buffering and electrical activity in mouse pancreatic beta-cells. *Biophys. J.* 76:2018–2028. doi:10.1016/S0006-3495(99)77359-5

Gilon, P., and J.C. Henquin. 1992. Influence of membrane potential changes on cytoplasmic Ca^{2+} concentration in an electrically excitable cell, the insulin-secreting pancreatic B-cell. *J. Biol. Chem.* 267:20713–20720.

Gilon, P., J. Yakel, J. Gromada, Y. Zhu, J.C. Henquin, and P. Rorsman. 1997. G protein-dependent inhibition of L-type Ca^{2+} currents by acetylcholine in mouse pancreatic B-cells. *J. Physiol.* 499:65–76.

Gilon, P., A. Arredouani, P. Gailly, J. Gromada, and J.C. Henquin. 1999. Uptake and release of Ca^{2+} by the endoplasmic reticulum contribute to the oscillations of the cytosolic Ca^{2+} concentration triggered by Ca^{2+} influx in the electrically excitable pancreatic B-cell. *J. Biol. Chem.* 274:20197–20205. doi:10.1074/jbc.274.29.20197

Goforth, P.B., R. Bertram, F.A. Khan, M. Zhang, A. Sherman, and L.S. Satin. 2002. Calcium-activated K^+ channels of mouse β-cells are controlled by both store and cytoplasmic Ca^{2+}: experimental and theoretical studies. *J. Gen. Physiol.* 120:307–322. doi:10.1085/jgp.20028581

Göpel, S.O., T. Kanno, S. Barg, L. Eliasson, J. Galvanovskis, E. Renström, and P. Rorsman. 1999a. Activation of Ca^{2+}-dependent K^+ channels contributes to rhythmic firing of action potentials in mouse pancreatic β cells. *J. Gen. Physiol.* 114:759–770. doi:10.1085/jgp.114.6.759

Göpel, S., T. Kanno, S. Barg, J. Galvanovskis, and P. Rorsman. 1999b. Voltage-gated and resting membrane currents recorded from B-cells in intact mouse pancreatic islets. *J. Physiol.* 521:717–728. doi:10.1111/j.1469-7793.1999.00717.x

Grapengiesser, E. 1996. Glucose induces cytoplasmic Na^+ oscillations in pancreatic beta-cells. *Biochem. Biophys. Res. Commun.* 226:830–835. doi:10.1006/bbrc.1996.1436

Grapengiesser, E. 1998. Unmasking of a periodic Na^+ entry into glucose-stimulated pancreatic beta-cells after partial inhibition of the Na/K pump. *Endocrinology.* 139:3227–3231. doi:10.1210/en.139.7.3227

Hao, L., J.L. Rigaud, and G. Inesi. 1994. Ca^{2+}/H^+ countertransport and electrogenicity in proteoliposomes containing erythrocyte plasma membrane Ca-ATPase and exogenous lipids. *J. Biol. Chem.* 269:14268–14275.

Henquin, J.C. 1990. Role of voltage- and Ca^{2+}-dependent K^+ channels in the control of glucose-induced electrical activity in pancreatic B-cells. *Pflugers Arch.* 416:568–572. doi:10.1007/BF00382691

Henquin, J.C., and H.P. Meissner. 1984a. Effects of theophylline and dibutyryl cyclic adenosine monophosphate on the membrane potential of mouse pancreatic beta-cells. *J. Physiol.* 351:595–612.

Henquin, J.C., and H.P. Meissner. 1984b. Significance of ionic fluxes and changes in membrane potential for stimulus-secretion coupling in pancreatic B-cells. *Experientia.* 40:1043–1052. doi:10.1007/BF01971450

Henquin, J.C., H.P. Meissner, and W. Schmeer. 1982. Cyclic variations of glucose-induced electrical activity in pancreatic B cells. *Pflugers Arch.* 393:322–327. doi:10.1007/BF00581418

Henquin, J.C., M. Nenquin, M.A. Ravier, and A. Szollosi. 2009. Shortcomings of current models of glucose-induced insulin secretion. *Diabetes Obes. Metab.* 11:168–179. doi:10.1111/j.1463-1326.2009.01109.x

Herchuelz, A., A. Kamagate, H. Ximenes, and F. Van Eylen. 2007. Role of Na/Ca exchange and the plasma membrane Ca^{2+}-ATPase in beta cell function and death. *Ann. NY Acad. Sci.* 1099:456–467. doi:10.1196/annals.1387.048

Herrington, J., M. Sanchez, D. Wunderler, L. Yan, R.M. Bugianesi, I.E. Dick, S.A. Clark, R.M. Brochu, B.T. Priest, M.G. Kohler, and O.B. McManus. 2005. Biophysical and pharmacological properties of the voltage-gated potassium current of human pancreatic beta-cells. *J. Physiol.* 567:159–175. doi:10.1113/jphysiol.2005.089375

Himeno, Y., F. Toyoda, H. Satoh, A. Amano, C.Y. Cha, H. Matsuura, and A. Noma. 2011. Minor contribution of cytosolic Ca^{2+} transients to the pacemaker rhythm in guinea pig sinoatrial node cells. *Am. J. Physiol. Heart Circ. Physiol.* 300:H251–H261. doi:10.1152/ajpheart.00764.2010

Hiriart, M., and D.R. Matteson. 1988. Na channels and two types of Ca channels in rat pancreatic B cells identified with the reverse hemolytic plaque assay. *J. Gen. Physiol.* 91:617–639. doi:10.1085/jgp.91.5.617

Hirschberg, B., J. Maylie, J.P. Adelman, and N.V. Marrion. 1998. Gating of recombinant small-conductance Ca-activated K^+ channels by calcium. *J. Gen. Physiol.* 111:565–581. doi:10.1085/jgp.111.4.565

Hopkins, W.F., S. Fatherazi, B. Peter-Riesch, B.E. Corkey, and D.L. Cook. 1992. Two sites for adenine-nucleotide regulation of ATP-sensitive potassium channels in mouse pancreatic beta-cells and HIT cells. *J. Membr. Biol.* 129:287–295.

Hoth, M., and R. Penner. 1993. Calcium release-activated calcium current in rat mast cells. *J. Physiol.* 465:359–386.

Houamed, K.M., I.R. Sweet, and L.S. Satin. 2010. BK channels mediate a novel ionic mechanism that regulates glucose-dependent electrical activity and insulin secretion in mouse pancreatic β-cells. *J. Physiol.* 588:3511–3523. doi:10.1113/jphysiol.2009.184341

Islam, M.S., O. Larsson, T. Nilsson, and P.O. Berggren. 1995. Effects of caffeine on cytoplasmic free Ca^{2+} concentration in pancreatic beta-cells are mediated by interaction with ATP-sensitive K^+ channels and L-type voltage-gated Ca^{2+} channels but not the ryanodine receptor. *Biochem. J.* 306:679–686.

Jacobson, D.A., F. Mendez, M. Thompson, J. Torres, O. Cochet, and L.H. Philipson. 2010. Calcium-activated and voltage-gated potassium channels of the pancreatic islet impart distinct and complementary roles during secretagogue induced electrical responses. *J. Physiol.* 588:3525–3537. doi:10.1113/jphysiol.2010.190207

Kanno, T., P. Rorsman, and S.O. Göpel. 2002. Glucose-dependent regulation of rhythmic action potential firing in pancreatic beta-cells by K_{ATP}-channel modulation. *J. Physiol.* 545:501–507. doi:10.1113/jphysiol.2002.031344

Keizer, J., and G. Magnus. 1989. ATP-sensitive potassium channel and bursting in the pancreatic beta cell. A theoretical study. *Biophys. J.* 56:229–242. doi:10.1016/S0006-3495(89)82669-4

Kelly, R.P., R. Sutton, and F.M. Ashcroft. 1991. Voltage-activated calcium and potassium currents in human pancreatic beta-cells. *J. Physiol.* 443:175–192.

Kinard, T.A., G. de Vries, A. Sherman, and L.S. Satin. 1999. Modulation of the bursting properties of single mouse pancreatic beta-cells by artificial conductances. *Biophys. J.* 76:1423–1435. doi:10.1016/S0006-3495(99)77303-0

Kukuljan, M., A.A. Goncalves, and I. Atwater. 1991. Charybdotoxin-sensitive $K_{(Ca)}$ channel is not involved in glucose-induced electrical activity in pancreatic beta-cells. *J. Membr. Biol.* 119:187–195. doi:10.1007/BF01871418

Larsson, O., H. Kindmark, R. Brandstrom, B. Fredholm, and P.O. Berggren. 1996. Oscillations in K_{ATP} channel activity promote oscillations in cytoplasmic free Ca^{2+} concentration in the pancreatic beta cell. *Proc. Natl. Acad. Sci. USA.* 93:5161–5165. doi:10.1073/pnas.93.10.5161

Leech, C.A., and J.F. Habener. 1998. A role for Ca^{2+}-sensitive nonselective cation channels in regulating the membrane potential of pancreatic beta-cells. *Diabetes.* 47:1066–1073. doi:10.2337/diabetes.47.7.1066

Lytton, J., M. Westlin, S.E. Burk, G.E. Shull, and D.H. MacLennan. 1992. Functional comparisons between isoforms of the sarcoplasmic or endoplasmic reticulum family of calcium pumps. *J. Biol. Chem.* 267:14483–14489.

MacDonald, P.E., A.M. Salapatek, and M.B. Wheeler. 2003. Temperature and redox state dependence of native Kv2.1 currents in rat pancreatic beta-cells. *J. Physiol.* 546:647–653. doi:10.1113/jphysiol.2002.035709

Magnus, G., and J. Keizer. 1998. Model of beta-cell mitochondrial calcium handling and electrical activity. I. Cytoplasmic variables. *Am. J. Physiol.* 274:C1158–C1173.

Marigo, V., K. Courville, W.H. Hsu, J.M. Feng, and H. Cheng. 2009. TRPM4 impacts on Ca^{2+} signals during agonist-induced insulin secretion in pancreatic beta-cells. *Mol. Cell. Endocrinol.* 299:194–203. doi:10.1016/j.mce.2008.11.011

Mears, D., N.F. Sheppard Jr., I. Atwater, E. Rojas, R. Bertram, and A. Sherman. 1997. Evidence that calcium release-activated current mediates the biphasic electrical activity of mouse pancreatic beta-cells. *J. Membr. Biol.* 155:47–59. doi:10.1007/s002329900157

Meissner, H.P., and H. Schmelz. 1974. Membrane potential of beta-cells in pancreatic islets. *Pflugers Arch.* 351:195–206. doi:10.1007/BF00586918

Merrins, M.J., B. Fendler, M. Zhang, A. Sherman, R. Bertram, and L.S. Satin. 2010. Metabolic oscillations in pancreatic islets depend on the intracellular Ca^{2+} level but not Ca^{2+} oscillations. *Biophys. J.* 99:76–84. doi:10.1016/j.bpj.2010.04.012

Meyer-Hermann, M.E. 2007. The electrophysiology of the beta-cell based on single transmembrane protein characteristics. *Biophys. J.* 93:2952–2968. doi:10.1529/biophysj.107.106096

Misler, S., L.C. Falke, K. Gillis, and M.L. McDaniel. 1986. A metabolite-regulated potassium channel in rat pancreatic B cells. *Proc. Natl. Acad. Sci. USA.* 83:7119–7123. doi:10.1073/pnas.83.18.7119

Miura, Y., J.C. Henquin, and P. Gilon. 1997. Emptying of intracellular Ca^{2+} stores stimulates Ca^{2+} entry in mouse pancreatic beta-cells by both direct and indirect mechanisms. *J. Physiol.* 503:387–398. doi:10.1111/j.1469-7793.1997.387bh.x

Miwa, Y., and Y. Imai. 1999. Simulation of spike-burst generation and Ca^{2+} oscillation in pancreatic beta-cells. *Jpn. J. Physiol.* 49:353–364. doi:10.2170/jjphysiol.49.353

Oka, C., C.Y. Cha, and A. Noma. 2010. Characterization of the cardiac Na^+/K^+ pump by development of a comprehensive and mechanistic model. *J. Theor. Biol.* 265:68–77. doi:10.1016/j.jtbi.2010.04.028

Owada, S., O. Larsson, P. Arkhammar, A.I. Katz, A.V. Chibalin, P.O. Berggren, and A.M. Bertorello. 1999. Glucose decreases Na^+,K^+-ATPase activity in pancreatic beta-cells. An effect mediated via Ca^{2+}-independent phospholipase A2 and protein kinase C-dependent phosphorylation of the alpha-subunit. *J. Biol. Chem.* 274:2000–2008. doi:10.1074/jbc.274.4.2000

Plant, T.D. 1988. Properties and calcium-dependent inactivation of calcium currents in cultured mouse pancreatic B-cells. *J. Physiol.* 404:731–747.

Prakriya, M., and R.S. Lewis. 2002. Separation and characterization of currents through store-operated CRAC channels and Mg^{2+}-inhibited cation (MIC) channels. *J. Gen. Physiol.* 119:487–507. doi:10.1085/jgp.20028551

Ribalet, B., and P.M. Beigelman. 1980. Calcium action potentials and potassium permeability activation in pancreatic beta-cells. *Am. J. Physiol.* 239:C124–C133.

Roe, M.W., L.H. Philipson, C.J. Frangakis, A. Kuznetsov, R.J. Mertz, M.E. Lancaster, B. Spencer, J.F. Worley III, and I.D. Dukes. 1994.

Defective glucose-dependent endoplasmic reticulum Ca^{2+} sequestration in diabetic mouse islets of Langerhans. *J. Biol. Chem.* 269:18279–18282.

Rorsman, P., and G. Trube. 1985. Glucose dependent K^+-channels in pancreatic beta-cells are regulated by intracellular ATP. *Pflugers Arch.* 405:305–309. doi:10.1007/BF00595682

Rorsman, P., and G. Trube. 1986. Calcium and delayed potassium currents in mouse pancreatic beta-cells under voltage-clamp conditions. *J. Physiol.* 374:531–550.

Rorsman, P., H. Abrahamsson, E. Gylfe, and B. Hellman. 1984. Dual effects of glucose on the cytosolic Ca^{2+} activity of mouse pancreatic beta-cells. *FEBS Lett.* 170:196–200. doi:10.1016/0014-5793(84)81398-8

Rorsman, P., P. Arkhammar, and P.O. Berggren. 1986. Voltage-activated Na^+ currents and their suppression by phorbol ester in clonal insulin-producing RINm5F cells. *Am. J. Physiol.* 251:C912–C919.

Rorsman, P., C. Ämmälä, P.O. Berggren, K. Bokvist, and O. Larsson. 1992. Cytoplasmic calcium transients due to single action potentials and voltage-clamp depolarizations in mouse pancreatic B-cells. *EMBO J.* 11:2877–2884.

Santos, R.M., and E. Rojas. 1989. Muscarinic receptor modulation of glucose-induced electrical activity in mouse pancreatic B-cells. *FEBS Lett.* 249:411–417. doi:10.1016/0014-5793(89)80669-6

Santos, R.M., L.M. Rosario, A. Nadal, J. Garcia-Sancho, B. Soria, and M. Valdeolmillos. 1991. Widespread synchronous $[Ca^{2+}]_i$ oscillations due to bursting electrical activity in single pancreatic islets. *Pflugers Arch.* 418:417–422. doi:10.1007/BF00550880

Satin, L.S., and D.L. Cook. 1989. Calcium current inactivation in insulin-secreting cells is mediated by calcium influx and membrane depolarization. *Pflugers Arch.* 414:1–10. doi:10.1007/BF00585619

Satin, L.S., W.F. Hopkins, S. Fatherazi, and D.L. Cook. 1989. Expression of a rapid, low-voltage threshold K current in insulin-secreting cells is dependent on intracellular calcium buffering. *J. Membr. Biol.* 112:213–222. doi:10.1007/BF01870952

Schulla, V., E. Renström, R. Feil, S. Feil, I. Franklin, A. Gjinovci, X.J. Jing, D. Laux, I. Lundquist, M.A. Magnuson, et al. 2003. Impaired insulin secretion and glucose tolerance in beta cell-selective $Ca_v1.2$ Ca^{2+} channel null mice. *EMBO J.* 22:3844–3854. doi:10.1093/emboj/cdg389

Sherman, A., J. Rinzel, and J. Keizer. 1988. Emergence of organized bursting in clusters of pancreatic beta-cells by channel sharing. *Biophys. J.* 54:411–425. doi:10.1016/S0006-3495(88)82975-8

Sherman, A., J. Keizer, and J. Rinzel. 1990. Domain model for Ca^{2+}-inactivation of Ca^{2+} channels at low channel density. *Biophys. J.* 58:985–995. doi:10.1016/S0006-3495(90)82443-7

Smith, P.A., P. Rorsman, and F.M. Ashcroft. 1989. Modulation of dihydropyridine-sensitive Ca^{2+} channels by glucose metabolism in mouse pancreatic beta-cells. *Nature.* 342:550–553. doi:10.1038/342550a0

Smith, P.A., F.M. Ashcroft, and P. Rorsman. 1990a. Simultaneous recordings of glucose dependent electrical activity and ATP-regulated K^+-currents in isolated mouse pancreatic beta-cells. *FEBS Lett.* 261:187–190. doi:10.1016/0014-5793(90)80667-8

Smith, P.A., K. Bokvist, P. Arkhammar, P.O. Berggren, and P. Rorsman. 1990b. Delayed rectifying and calcium-activated K^+ channels and their significance for action potential repolarization in mouse pancreatic β-cells. *J. Gen. Physiol.* 95:1041–1059. doi:10.1085/jgp.95.6.1041

Smolen, P. 1995. A model for glycolytic oscillations based on skeletal muscle phosphofructokinase kinetics. *J. Theor. Biol.* 174:137–148. doi:10.1006/jtbi.1995.0087

Smolen, P., and J. Keizer. 1992. Slow voltage inactivation of Ca^{2+} currents and bursting mechanisms for the mouse pancreatic beta-cell. *J. Membr. Biol.* 127:9–19.

Sturgess, N.C., C.N. Hales, and M.L. Ashford. 1987. Calcium and ATP regulate the activity of a non-selective cation channel in a rat insulinoma cell line. *Pflugers Arch.* 409:607–615. doi:10.1007/BF00584661

Takeuchi, A., S. Tatsumi, N. Sarai, K. Terashima, S. Matsuoka, and A. Noma. 2006. Ionic mechanisms of cardiac cell swelling induced by blocking Na^+/K^+ pump as revealed by experiments and simulation. *J. Gen. Physiol.* 128:495–507. doi:10.1085/jgp.200609646

Tamarina, N.A., Y. Wang, L. Mariotto, A. Kuznetsov, C. Bond, J. Adelman, and L.H. Philipson. 2003. Small-conductance calcium-activated K^+ channels are expressed in pancreatic islets and regulate glucose responses. *Diabetes.* 52:2000–2006. doi:10.2337/diabetes.52.8.2000

Tengholm, A., B. Hellman, and E. Gylfe. 2001. The endoplasmic reticulum is a glucose-modulated high-affinity sink for Ca^{2+} in mouse pancreatic beta-cells. *J. Physiol.* 530:533–540. doi:10.1111/j.1469-7793.2001.0533k.x

Tse, F.W., A. Tse, and B. Hille. 1994. Cyclic Ca^{2+} changes in intracellular stores of gonadotropes during gonadotropin-releasing hormone-stimulated Ca^{2+} oscillations. *Proc. Natl. Acad. Sci. USA.* 91:9750–9754. doi:10.1073/pnas.91.21.9750

Váradi, A., E. Molnár, and S.J. Ashcroft. 1995. Characterisation of endoplasmic reticulum and plasma membrane Ca^{2+}-ATPases in pancreatic beta-cells and in islets of Langerhans. *Biochim. Biophys. Acta.* 1236:119–127. doi:10.1016/0005-2736(95)00103-A

Váradi, A., E. Molnár, C.G. Ostenson, and S.J. Ashcroft. 1996. Isoforms of endoplasmic reticulum Ca^{2+}-ATPase are differentially expressed in normal and diabetic islets of Langerhans. *Biochem. J.* 319:521–527.

Velasco, J.M., and O.H. Petersen. 1987. Voltage-activation of high-conductance K^+ channel in the insulin-secreting cell line RINm5F is dependent on local extracellular Ca2+ concentration. *Biochim. Biophys. Acta.* 896:305–310. doi:10.1016/0005-2736(87)90191-X

Vignali, S., V. Leiss, R. Karl, F. Hofmann, and A. Welling. 2006. Characterization of voltage-dependent sodium and calcium channels in mouse pancreatic A- and B-cells. *J. Physiol.* 572:691–706.

Worley, J.F., III, M.S. McIntyre, B. Spencer, and I.D. Dukes. 1994a. Depletion of intracellular Ca^{2+} stores activates a maitotoxin-sensitive nonselective cationic current in beta-cells. *J. Biol. Chem.* 269:32055–32058.

Worley, J.F., III, M.S. McIntyre, B. Spencer, R.J. Mertz, M.W. Roe, and I.D. Dukes. 1994b. Endoplasmic reticulum calcium store regulates membrane potential in mouse islet beta-cells. *J. Biol. Chem.* 269:14359–14362.

Zhang, M., P. Goforth, R. Bertram, A. Sherman, and L. Satin. 2003. The Ca^{2+} dynamics of isolated mouse beta-cells and islets: implications for mathematical models. *Biophys. J.* 84:2852–2870. doi:10.1016/S0006-3495(03)70014-9

Zhang, M., K. Houamed, S. Kupershmidt, D. Roden, and L.S. Satin. 2005. Pharmacological properties and functional role of K_{slow} current in mouse pancreatic β-cells: SK channels contribute to K_{slow} tail current and modulate insulin secretion. *J. Gen. Physiol.* 126:353–363. doi:10.1085/jgp.200509312

Utility of indices using C-peptide levels for indication of insulin therapy to achieve good glycemic control in Japanese patients with type 2 diabetes

Shogo Funakoshi[1], Shimpei Fujimoto[1]*, Akihiro Hamasaki[1], Hideya Fujiwara[1], Yoshihito Fujita[1], Kaori Ikeda[1], Shiho Takahara[1], Kazuaki Nagashima[1], Masaya Hosokawa[1], Yutaka Seino[2], Nobuya Inagaki[1]

ABSTRACT

Aims/Introduction: Type 2 diabetes is progressive in that therapy must be altered over time, which is partly as a result of the progressive loss of pancreatic β-cell function. To elucidate the relationship between residual endogenous insulin secretion and the necessity of insulin therapy to achieve good glycemic control, indices using serum C-peptide immunoreactivity (CPR) were analyzed in patients with type 2 diabetes.

Materials and Methods: The data of 201 Japanese patients with type 2 diabetes who achieved the target of glycemic control during admission were analyzed retrospectively. Indices using CPR including fasting CPR (FCPR), CPR 6 min after intravenous injection of glucagon (CPR-6 min), increment of CPR (ΔCPR), secretory unit of islet in transplantation index (SUIT) and C-peptide index (CPI) were compared between the group requiring insulin (insulin group) and the group not requiring insulin (non-insulin group). A receiver–operator characteristic (ROC) curve was made, and optimal cut-off point and likelihood ratio were determined for each index.

Results: All indices of CPR were lower in the insulin group compared with those in the non-insulin group. Likelihood ratios at the optimal point of FCPR, CPR-6 min, ΔCPR, SUIT, and CPI were 2.0, 2.1, 1.6, 2.3 and 2.8, respectively. Optimal cut-off point of CPI was 1.1 ng/mg. Sensitivity and specificity at optimal point of CPI were 61 and 78%, respectively.

Conclusions: The advantage of CPI of the indices of CPR to select insulin therapy to achieve good glycemic control was shown, but limitations of the predictive abilities of the indices using CPR should be taken into account. (J Diabetes Invest, doi: 10.1111/j.2040-1124.2010.00096.x, 2011)

KEY WORDS: C-peptide, Insulin therapy, Glycemic control

INTRODUCTION

Type 2 diabetes is a heterogeneous disease characterized by insulin resistance and defective insulin secretion[1], and is progressive in that therapy must be altered over time. Initially on diagnosis, diet and exercise are generally adequate to achieve good glycemic control; oral hypoglycemic agents (OHA) are required later, when patients cannot achieve control with diet and exercise alone. Daily insulin injection is indicated when patients are unable to achieve control with a combination of oral agents, diet and exercise[2,3]. Insulin therapy is required in these patients not for survival, as is found in type 1 diabetes, but for good glycemic control[4]. This requirement is, at least in part, as a result of the progressive loss of pancreatic β-cell function. The results of the United Kingdom Progressive Diabetes Study (UKPDS) shows that pancreatic β-cell function (%β), assessed by Homeostasis Model Assessment (HOMA) in patients allocated to diet or OHA, decreased approximately 25% in 5 years[5]. A decline in endogenous insulin secretion over more than several decades of diabetes was observed in a cross-sectional study[6].

Determination of fasting serum C-peptide level and stimulated serum C-peptide level by intravenous glucagon is used widely to assess endogenous insulin secretory reserves[7–10]. There are several reports regarding the correlation between levels of residual endogenous insulin secretion and the choice of insulin therapy to achieve glycemic control[11–14]. However, in these studies, because the glycemic goal was not described clearly or was inappropriate, patients with insufficient glycemic control by the selected mode of therapy were sometimes included.

[1]Department of Diabetes and Clinical Nutrition, Graduate School of Medicine, Kyoto University, Kyoto, and [2]Kansai Electric Power Hospital, Osaka, Japan
*Corresponding author. Shimpei Fujimoto Tel.: +81-75-751-3560
Fax: +81-75-751-4244 E-mail address: fujimoto@metab.kuhp.kyoto-u.ac.jp
Received 9 September 2010; revised 12 November 2010; accepted 24 November 2010

In the present study, to evaluate the clinical significance of measures of serum C-peptide in achieving good glycemic control, we retrospectively analyzed the use of indices of endogenous insulin secretion in type 2 diabetes patients admitted to our hospital. Using data of patients who achieved the target of glycemic control during the period of admission, the patients were divided into two groups: one that achieved good control without the use of insulin (non-insulin group) and the other that required the use of insulin (insulin group), and the indices using serum C-peptide were compared between them. Optimal values and the utility of indices using serum C-peptide to select insulin therapy to achieve good glycemic control were analyzed.

MATERIALS AND METHODS

Subjects

A total of 746 Japanese patients with type 2 diabetes admitted between 2003 and 2009 to Kyoto University Hospital for poor glycemic control were enrolled in the present study. Type 2 diabetes mellitus was diagnosed based on the criteria of the American Diabetes Association (ADA)[15]. As indicated in Figure S1, 76 patients including those with pancreatic disease and liver disease, those taking diabetogenic medication and pregnant women were excluded. A total of 40 patients with incomplete clinical examinations also were excluded, and 66 patients with serum creatinine ≥1.3 mg/dL were excluded, as serum C-peptide immunoreactivity (CPR) is elevated by decreased renal function[16]. The data of 90 patients taking oral hypoglycemic agents (OHA) plus insulin at discharge were excluded. Good control was defined as mean preprandial capillary plasma glucose level <130 mg/dL, according to the glycemic control recommendation of ADA[17]. The 474 patients were divided into two groups: 201 patients who achieved good glycemic control (achieved group) and 273 patients who did not (non-achieved group). As shown in Figure S2, of the 201 patients in the achieved group, 47, 107, 38 and nine patients were treated with diet alone, OHA, insulin and insulin plus OHA at admission, respectively. At discharge, 24, 95 and 82 patients were treated with diet alone, OHA and insulin, respectively. Patients treated with diet alone and OHA at discharge comprised the non-insulin group; patients treated with insulin at discharge comprised the insulin group. A total of 166 patients of the 474 patients in the achieved or non-achieved group at discharge who could be confirmed within 6 months after discharge to achieve <7.4% in HbA_{1c}, which excludes 'not good' and 'poor' for assessment of glycemic control in the treatment guide for diabetes of the Japan Diabetes Society (JDS guide)[18], were re-analyzed to determine the cut-off point for C-peptide index (CPI) for longer duration of glycemic control. Of the 201 patients in the achieved group at discharge, 85 were excluded as a result of readmission or alteration to the mode of therapy, or were not followed as outpatients due to a change of hospital. Of the remaining 116 patients, 90 showed <7.4% HbA_{1c} within 6 months after discharge. Of the 273 patients in the non-achieved group at discharge, 137 were excluded as a result of readmission or alteration to the mode of therapy, or were not followed as outpatients due to a change of hospital. In the remaining 136 patients, 76 achieved <7.4% HbA_{1c} within 6 months after discharge. In these 166 patients, analysis of optimal values and the utility of CPI during admission was carried out.

Methods

On the first day in hospital, medical history, physical examination and laboratory evaluation including glycosylated hemoglobin were carried out. HbA_{1c} was measured using HPLC (HA-8180; Arcray, Kyoto, Japan). The HbA_{1c} (%) value was estimated as an National Glycohemoglobin Standardization Program equivalent (%) calculated by the formula: HbA_{1c} (%) = HbA_{1c} (JDS) (%) + 0.4%, considering the relational expression of HbA_{1c} (JDS) (%) measured by the previous Japanese standard substance and measurement methods and HbA_{1c} (National Glycohemoglobin Standardization Program)[19]. β-cell function was evaluated within 1 week after overnight fast by glucagon test measuring CPR before (fasting CPR [FCPR]) and 6 min after i.v. injection of 1 mg glucagon (CPR-6 min)[7], as this test is valid in patients taking insulin therapy. Increment of CPR (ΔCPR) was obtained by subtracting FCPR from CPR-6 min. SUIT index (SUIT) (%) was calculated by the formula: 1500 × FCPR (ng/mL)/(fasting plasma glucose [FPG; mg/dL] − 61.7)[20]. CPI (ng/mg) was calculated by the formula: 100 × FCPR (ng/mL)/FPG (mg/dL). Serum CPR was measured by immunoenzymometric assay (EIA; ST AIA-PACK C-Peptide, Toso corporation, Tokyo, Japan). In patients taking OHA, medication was stopped for the glucagon test, but was maintained until 1 day before to prevent hyperglycemia during the test[6]. Fasting plasma glucose was measured by the glucose oxidase method when the glucagon test was carried out. Patients were treated according to the JDS guide[18]. Treatment policy including diet therapy, exercise therapy, pharmacotherapy and education for each patient was determined by Japanese Board Certified Diabetologists certified by the Japan Diabetes Society. Patients took medical nutritional therapy (25–30 kcal/kg of standard bodyweight/day consisting of 58% carbohydrate, 18% protein and 24% fat energy intake percentages) with counseling by a registered dietitian. Preprandial capillary plasma glucose levels were monitored three t.i.d. during hospitalization. The study protocol was approved by the ethics committee of Kyoto University.

Statistical analysis

Statistical analysis was carried out with the Stat View 5.0 system (SAS institute, Cary, NC, USA). Data are presented as mean ± SE unless otherwise stated. Clinical parameters among the two groups were compared by Mann–Whitney *U*-test. *P*-values <0.01 were considered statistically significant. Histograms and receiver–operator characteristic (ROC) curve were made for FCPR, CPR-6 min, ΔCPR, SUIT and CPI respectively, and sensitivity, specificity, cut-off values, area under the ROC curve (AUC) and the likelihood ratio were calculated.

RESULTS

Clinical profiles of patients with mean preprandial capillary plasma glucose levels at discharge of <130 mg/dL (achieved group) and ≥130 mg/dL (non-achieved group), respectively, are shown in Table 1. Patients of the non-achieved group were older, had lower body mass index at admission, higher mean preprandial capillary plasma glucose level both at admission and at discharge, longer years from diagnosis and lower endogenous insulin secretion indices than those of the achieved group. The clinical stages of diabetic nephropathy and retinopathy were more progressed in the non-achieved group than those in the achieved group. The relationships between indices using serum C-peptide and selected modes of therapy at discharge were analyzed based on the data of the achieved group.

The clinical profiles of patients not requiring insulin for good glycemic control (non-insulin group) and those requiring insulin (insulin group) are shown in Table 2. The patients of the insulin group were older, has lower body mass index, higher HbA_{1c} at admission, higher mean preprandial capillary plasma glucose level at admission, longer years from diagnosis and lower endogenous insulin secretion indices compared with those of the non-insulin group. As shown in Figure S2, the mode of therapy in 41 patients was altered from diet alone or OHA to insulin during admission. The average number of hospital days before altering the therapeutic mode of these patients was 3.1 ± 3.4 (mean ± SD). The reasons for the change to insulin therapy were the necessity of tight glycemic control before operation in five patients, marked hyperglycemia (a fasting plasma glucose level of 250 mg/dL or above, or a causal plasma glucose of 350 mg/dL or above)[21] or both the presence of hyperglycemia and ketosis in 11 patients, and persistent hyperglycemia with OHA in 25 patients. HbA_{1c} at admission of these patients was 10.2 ± 2.2% (mean ± SD). In five patients, the mode of therapy was altered from insulin to OHA. The average number of hospital days before this change was 7.6 ± 4.3 (mean ± SD); the reason was improved glycemic control despite a decrease in the required dosage of insulin. HbA_{1c} at admission of these patients was 10.1 ± 4.4% (mean ± SD). Another patient treated with OHA plus insulin at admission was changed to OHA alone after nine hospital days because of improved glycemic control. Of the 113 patients with therapy of diet alone or OHA both at admission and at discharge, 19 transiently used insulin during the period of admission.

The category of OHA at discharge is shown in Table S1a. In 95 patients treated with OHA, 60 and 29 patients were prescribed sulfonylurea alone or in combination, and biguanide alone or in combination, respectively. In the insulin group, 50 of 86 patients were given premixed insulin b.i.d. at discharge. As shown in Table S1b, the prescribed daily dosages of gliclazide, glimepiride and metformin required were <80, 4 and 750 mg,

Table 1 | Clinical profiles of patients who achieved good glycemic control

	Achieved	Non-achieved	*P*
No. subjects	201	273	
Duration of hospitalization (days)	22.0 ± 0.7	23.6 ± 0.7	0.1115
Age (years)	60.2 ± 0.9	64.5 ± 0.7*	0.0002
Male/female	127/74	159/114	
Systolic blood pressure (mmHg)	124.5 ± 1.0	126.9 ± 1.1	0.1076
Diastolic blood pressure (mmHg)	74.6 ± 0.7	73.6 ± 0.6	0.2653
BMI (kg/m^2)	25.2 ± 0.3	23.8 ± 0.3*	0.0005
HbA_{1c} at admission (%)	9.5 ± 0.1	9.8 ± 0.1	0.0776
PG at admission (mg/dL)	181.1 ± 4.7	209.5 ± 3.9*	<0.0001
PG at discharge (mg/dL)	112.2 ± 0.9	163.2 ± 1.9*	<0.0001
Years from diagnosis	9.1 ± 0.6	13.5 ± 0.6*	<0.0001
FCPR (ng/mL)	1.87 ± 0.06	1.65 ± 0.05*	0.0054
CPR-6 min (ng/mL)	3.99 ± 0.14	3.41 ± 0.10*	0.0006
ΔCPR (ng/mL)	2.12 ± 0.09	1.76 ± 0.07*	0.0011
SUIT (%)	40.6 ± 1.9	32.4 ± 2.0*	0.0043
CPI (ng/mg)	1.34 ± 0.05	1.09 ± 0.04*	<0.0001
Clinical stage of nephropathy (normal/microalbuminuria/macroalbuminuria)	129/56/16 (64/28/8)	133/80/60 (49/29/22)	
Clinical stage of retinopathy (NDR/mild NPDR/moderate NPDR/severe NPDR/PDR)	141/25/26/4/5 (71/12/13/2/2)	112/53/45/22/41 (41/20/16/8/15)	

Data are presented as mean ± SE. *$P < 0.01$ versus achieved. Achieved group: mean preprandial capillary plasma glucose levels at discharge <130 mg/dL compared with those who did not achieve good glycemic control (non-achieved group ≥130 mg/dL). BMI, body mass index; CPI, C-peptide index; ΔCPR, increment of C-peptide immunoreactivity; CPR-6 min, C-peptide immunoreactivity 6 min after intravenous injection of glucagon; FCPR, fasting C-peptide immunoreactivity; NDR, no diabetic retinopathy; NPDR, non-proliferative diabetic retinopathy; PDR, proliferative diabetic retinopathy; PG, mean preprandial capillary plasma glucose level; SUIT, secretory unit of islet in transplantation index. Numbers in parentheses indicate percentages.

Table 2 | Clinical profiles of patients who achieved good glycemic control without requiring the use of insulin and those requiring insulin to achieve good glycemic control

	Non-insulin	Insulin	*P*
No. subjects	119	82	
Male/female	82/37	45/37	
Age (years)	58.4 ± 1.1	62.9 ± 1.3*	0.0099
Systolic blood pressure (mmHg)	124.4 ± 1.4	126.4 ± 1.7	0.3598
Diastolic blood pressure (mmHg)	77.3 ± 1.0	73.3 ± 1.3	0.0135
BMI (kg/m^2)	26.0 ± 0.4	24.0 ± 0.4*	0.0019
HbA_{1c} at admission (%)	9.2 ± 0.2	10.0 ± 0.2*	0.0050
PG at admission (mg/dL)	163.2 ± 5.0	206.9 ± 8.0*	<0.0001
PG at discharge (mg/dL)	110.9 ± 1.2	114.2 ± 1.3	0.0602
Years from diagnosis	7.8 ± 0.6	10.9 ± 1.0*	0.0052
FCPR (ng/mL)	2.06 ± 0.07	1.61 ± 0.09*	0.0001
CPR-6 min (ng/mL)	4.48 ± 0.18	3.29 ± 0.19*	<0.0001
ΔCPR (ng/mL)	2.43 ± 0.12	1.68 ± 0.12*	<0.0001
SUIT (%)	47.2 ± 2.5	31.1 ± 2.7*	<0.0001
CPI (ng/mg)	1.57 ± 0.07	1.06 ± 0.06*	<0.0001

Data are presented as mean ± SE. *$P < 0.01$ versus non-insulin. Good glycemic control: mean preprandial capillary plasma glucose levels at discharge <130 mg/dL.
BMI, body mass index; CPI, C-peptide index; ΔCPR, increment of C-peptide immunoreactivity; CPR-6 min, C-peptide immunoreactivity 6 min after intravenous injection of glucagon; FCPR, fasting C-peptide immunoreactivity; PG, mean preprandial capillary plasma glucose level; SUIT, secretory unit of islet in transplantation index.

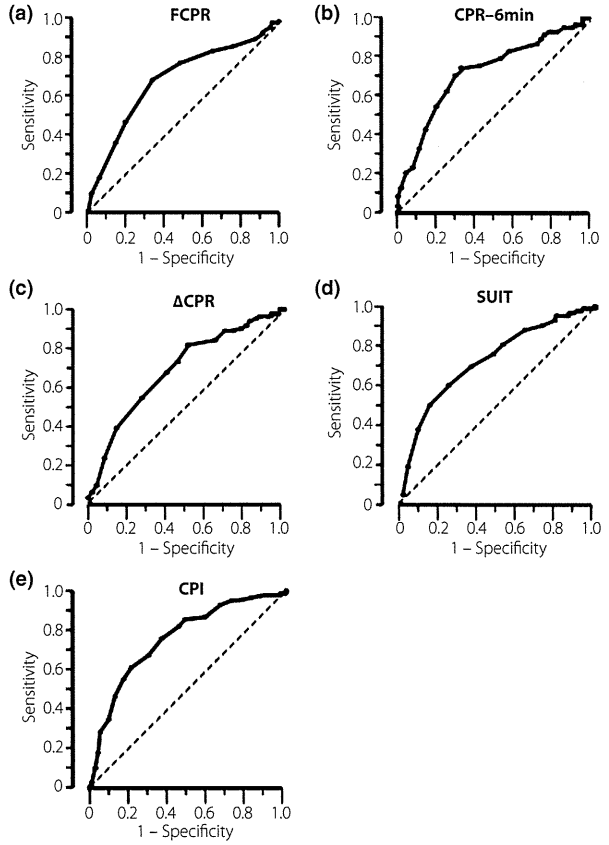

Figure 1 | Receiver–operator characteristic curves of (a) fasting C-peptide immunoreactivity (FCPR), (b) CPR 6 min after intravenous injection of glucagon (CPR-6 min), (c) increment of CPR (ΔCPR), (d) secretory unit of islet in transplantation index (SUIT) and (e) C-peptide index (CPI) of patients with mean preprandial capillary plasma glucose levels of <130 mg/dL at discharge.

respectively in almost all (more than 95%) patients. Daily insulin dosage was 22.0 ± 11.1 U (mean ± SD) in the insulin group.

In Figure S3, peak relative frequency of indices using CPR of patients with mean preprandial capillary plasma glucose levels of <130 mg/dL at discharge in the insulin group and the non-insulin group, respectively, is shown (FCPR: 1.50–1.75, 2.00–2.25 ng/mL; CPR-6 min: 2.75–3.00, 4.00–4.25 ng/mL; ΔCPR: 1.25–1.50, 1.25–1.50 plus 2.25–2.50 ng/mL; SUIT: 15–20, 25–30 plus 35–40 plus 45–50%; and CPI: 0.8–0.9, 1.5–1.6 ng/mg). According to ROC curves of indices using CPR shown in Figure 1, AUC, cut-off values and values at optimal cut-off points including sensitivity, specificity and the likelihood ratio were determined and shown in Table 3. CPI is the most relevant of these indices for selecting insulin therapy to achieve good glycemic control, because the likelihood ratio and AUC of CPI is greatest.

The ROC curve of CPI of patients who achieved <7.4% HbA_{1c} within 6 months after discharge is shown in Figure 2. According to ROC curves of CPI in Figure 2, the AUC (0.75), cut-off values (optimal: 1.2; 90% specificity 0.8; 90% sensitivity 1.7 ng/mg), and values at optimal cut-off points including sensitivity (73%), specificity (71%) and the likelihood ratio (2.5) were determined.

DISCUSSION

Medical nutritional therapy (MNT) improves glycemic control in patients with type 2 diabetes regardless of their modes of therapy including diet alone, OHA and insulin[22–24]. Diet therapy is the basis and starting point of treatment of all patients with diabetes[25], and failure of diet therapy alone might predict the inability to attain optimal glycemic control by any of these modes of therapy. To precisely analyze the relationship between endogenous insulin secretion and the appropriate mode of therapy for achieving good glycemic control, we used data of hospitalized patients under optimal therapy including proper MNT. Thus, our results are more likely to be valid in patients with appropriate care behaviors. Although inappropriate care behavior is an obstacle to achieving good glycemic control over a longer duration, our results suggest a basis for beginning insulin therapy in patients who do not achieve good glycemic control with diet alone or OHA despite the practice of appropriate care behavior.

Table 3 | Analysis of indices using serum C-peptide of patients with mean preprandial capillary plasma glucose levels of <130 mg/dL at discharge

	FCPR	CPR-6 min	ΔCPR	SUIT	CPI
AUC	0.69	0.71	0.69	0.72	0.75
Cut-off values	(ng/mL)	(ng/mL)	(ng/mL)	(%)	(ng/mg)
Optimal	1.75	3.75	2.25	30	1.1
90% Specificity	1.00	2.25	1.00	20	0.7
90% Sensitivity	2.75	5.25	3.25	55	1.7
Values at optimal cut-off points					
Sensitivity (%)	70	74	82	61	61
Specificity (%)	66	65	49	73	78
Likelihood ratio	2.0	2.1	1.6	2.3	2.8

AUC, area under receiver–operator characteristics curve; CPI, C-peptide index; ΔCPR, increment of C-peptide immunoreactivity; CPR-6 min, C-peptide immunoreactivity 6 min after intravenous injection of glucagon; FCPR, fasting C-peptide immunoreactivity; SUIT, secretory unit of islet in transplantation index

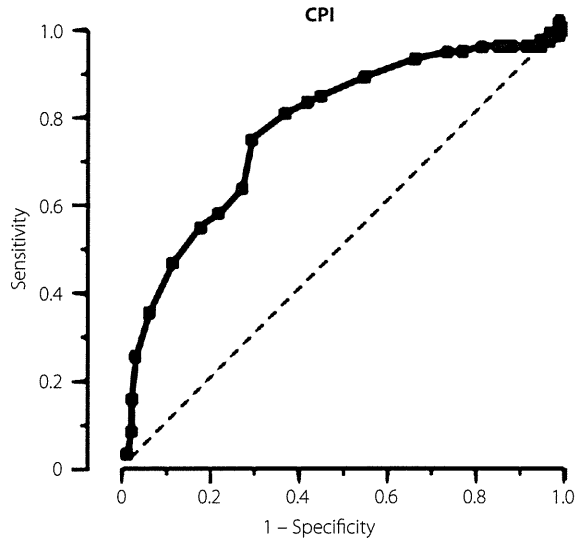

Figure 2 | Receiver–operator characteristic curve of C-peptide index (CPI) of patients who achieved <7.4% HbA_{1c} within 6 months after discharge.

In the present study, just 42% of patients achieved good control during hospital admission, partly because the aim of admission was not necessarily to achieve good control during the period of admission, but to establish a treatment policy for the achievement of good control after discharge. The percentage of patients treated with insulin at discharge was higher in the non-achieved group than in the achieved group (non-achieved group: 67%; achieved group: 41%). Of the patients treated with OHA at admission in the achieved group, 39% had therapy changed to insulin, whereas 73% of the patients treated with OHA at admission in the non-achieved group had therapy changed to insulin. These results might indicate more intensive therapy in the case of the non-achieved group. Of the 136 patients in the non-achieved group at discharge, 76 showed <7.4% HbA_{1c} within 6 months after discharge, showing fair glycemic control in some of the patients of this group over the longer term. As shown in Table 1, the non-achieved group had more progressive diabetic complications and more years from diagnosis compared with the achieved group. These factors might prompt therapy that aims at a more gradual improvement of glycemic control to prevent hypoglycemia. In addition, the non-achieved group showed higher glycemic levels at admission than that of the achieved group, whereas the duration of hospitalization was similar.

Although there have been several reports regarding the utility of indices of endogenous insulin secretion to indicate initiation of insulin therapy to improve glycemic control[11–14], none has compared the utility of the various indices. In the present study, as shown by the likelihood ratio and by AUC, CPI is shown to be the most useful among the five indices.

CPI was used as an index of endogenous insulin secretion in several reports[26–28], but its advantage over other indices and the scientific basis was unclear. The SUIT index (SUIT) was developed using FCPR and plasma glucose level after islet transplantation[19]. The linear relationship between FCPR and FPG in individual subjects shows a plasma glucose level (61.7 mg/dL) assumed to suppress C-peptide to zero. Transplantation of islets from non-diabetic donors increases the slope (FCPR/[FPG − 61.7]), suggesting an index of transplanted β-cell mass. Although a correlation between SUIT and CPR 6 min after intravenous injection of 1 mg glucagon (CPR-6 min) is observed in type 2 diabetes ($r = 0.58$), it is weaker than that in patients after islet transplantation ($r = 0.82$)[19].

Autopsy reveals that β-cell mass is decreased in patients with type 2 diabetes compared with that in healthy subjects[29–31]. Recently, in 33 subjects at various stages of glucose tolerance, a correlation between β-cell areas of a sample obtained during pancreatectomy, and serum levels of CPR and insulin before the operation was analyzed[32]. Interestingly, β-cell areas are positively correlated with fasting insulin/FPG ($r = 0.51$, $P = 0.0024$) and FCPR/FPG ($r = 0.63$, $P < 0.0001$), but are not significantly

correlated with homeostasis model assessment β-cell function (HOMA-β). Because SUIT resembles HOMA-β in that insulin secretion is assumed to be suppressed to zero at approximately 60 mg/dL glucose in the formula, CPI might be a better index of residual β-cell mass than SUIT in subjects with glucose intolerance. Furthermore, CPI is not affected by exogenous insulin[27], which might favor reproducibility of the results in patients with insulin therapy. Determination of the index using a one-point blood sample without the use of loading agents also favors CPI.

In results derived from CPI of patients with mean preprandial capillary plasma glucose levels of <130 mg/dL at discharge, AUC was 0.75, optimal cut-off value was 1.1 ng/mg with 61% sensitivity and 78% specificity, and values at 90% sensitivity and at 90% specificity were 1.7 and 0.7 ng/mg, respectively. Interestingly, in results derived from CPI of patients who achieved <7.4% HbA_{1c} within 6 months after discharge, AUC was 0.75, optimal cut-off value was 1.2 ng/mg with 73% sensitivity and 71% specificity, and values at 90% sensitivity and at 90% specificity were 1.7 and 0.8 ng/mg, respectively, similar to the values evaluated by mean preprandial glucose levels at discharge. These values are also similar to those in a previous report in Japanese using the data of 180 subjects from another institution (optimal cut-off value: 1.0 with 62% sensitivity and 81% specificity; values at 90% sensitivity: 1.8; 90% specificity: 0.7 ng/mg), although good glycemic control was defined as 8.4% in HbA_{1c}, which is somewhat inadequate[14]. Thus, CPI might be a predictor of suitable therapy to achieve fair glycemic control not only for the short-term, but also for longer duration.

The main limitation of the present study is that it is a retrospective analysis of inpatients at one hospital, and the protocol for starting insulin therapy was not defined precisely. However, in the achieved group analyzed as subjects, the decisions as to whether to start insulin therapy made by Japanese Board Certified Diabetologists were confirmed retrospectively to have been made according to the treatment guide for diabetes of the Japan Diabetes Society, as discussed in the results section.

In conclusion, we have shown the advantage of CPI of indices using CPR to select insulin therapy to achieve good glycemic control. However, limitations of the predictive abilities of indices using CPR generally and the importance of observation of the clinical therapeutic course must be taken into consideration.

ACKNOWLEDGEMENTS

The authors declare no conflict of interest.

REFERENCES

1. DeFronzo RA. Lilly lecture 1987. The triumvirate: β-cell, muscle, liver. A collusion responsible for NIDDM. *Diabetes* 1988; 37: 667–687.
2. Yki-Järvinen H, Kauppila M, Kujansuu E, *et al.* Comparison of insulin regimens in patients with non-insulin-dependent diabetes mellitus. *N Engl J Med* 1992; 327: 1426–1433.
3. Turner RC, Cull CA, Frighi V, *et al.* Glycemic control with diet, sulfonylurea, metformin, or insulin in patients with type 2 diabetes mellitus: progressive requirement for multiple therapies (UKPDS 49). UK Prospective Diabetes Study (UKPDS) Group. *JAMA* 1999; 281: 2005–2012.
4. Japan Diabetes Society. Diabetes mellitus: the disease itself. In: Japan Diabetes Society (ed.). *Treatment Guide for Diabetes 2007*. Bunkodo, Japan, 2007; 8–13.
5. U.K. Prospective Diabetes Study Group. U.K. prospective diabetes study 16. Overview of 6 years' therapy of type II diabetes: a progressive disease. *Diabetes* 1995; 44: 1249–1258.
6. Funakoshi S, Fujimoto S, Hamasaki A, *et al.* Analysis of factors influencing pancreatic β-cell function in Japanese patients with type 2 diabetes: association with body mass index and duration of diabetic exposure. *Diabetes Res Clin Pract* 2008; 82: 353–358.
7. Faber OK, Binder C. C-peptide response to glucagon. A test for the residual β-cell function in diabetes mellitus. *Diabetes* 1977; 26: 605–610.
8. Hendriksen C, Faber OK, Drejer J, *et al.* Prevalence of residual B-cell function in insulin-treated diabetics evaluated by the plasma C-peptide response to intravenous glucagon. *Diabetologia* 1977; 13: 615–619.
9. Jayyab AK, Heding LG, Czyzyk A, *et al.* Serum C peptide and IRI levels after administration of glucagon and glucose in non-insulin-dependent diabetics. *Horm Metab Res* 1982; 14: 112–116.
10. Gjessing HJ, Damsgaard EM, Matzen LE, *et al.* Reproducibility of β-cell function estimates in non-insulin-dependent diabetes mellitus. *Diabetes Care* 1987; 10: 558–562.
11. Madsbad S, Krarup T, McNair P, *et al.* Practical clinical value of the C-peptide response to glucagon stimulation in the choice of treatment in diabetes mellitus. *Acta Med Scand* 1981; 210: 153–156.
12. Sanke T, Satogami E, Sowa R, *et al.* Plasma C-peptide response during glucagon test as an index for evaluation of insulin requirement in diabetics (in Japanese). *J Jpn Diab Soc* 1985; 28: 713–719.
13. Koskinen P, Viikari J, Irjala K, *et al.* C-peptide determination in the choice of treatment in diabetes mellitus. *Scand J Clin Lab Invest* 1985; 45: 589–597.
14. Asano T, Kawamura M, Watanabe T, *et al.* Indices of urinary and serum C-peptide corrected with fasting plasma glucose for decision-making of insulin therapy in type 2 diabetes-validation and comparison (in Japanese). *J Jpn Diab Soc* 2008; 51: 759–763.
15. American Diabetes Association. Diagnosis and classification of diabetes mellitus. *Diabetes Care* 2010; 33: S62–S69.
16. Kajinuma H, Tanabashi S, Ishiwata K, *et al.* Urinary excretion of C-peptide in relation to renal function. In: Baba S (ed.). *Proinsulin, Insulin, C-Peptide*. Excerpta Medica, Amsterdam, 1979; 183–189.
17. American Diabetes Association. Standards of medical care in diabetes-2010. *Diabetes Care* 2010; 33: S11–S61.
18. Japan Diabetes Society (ed.). *Treatment Guide for Diabetes 2007*. Bunkodo, Japan, 2007.

19. The Committee of Japan Diabetes Society on the diagnostic criteria of diabetes mellitus. Report of the Committee on the classification and diagnostic criteria of diabetes mellitus. *J Diabetes Invest* 2010; 1: 212–228.
20. Yamada Y, Fukuda K, Fujimoto S, *et al.* SUIT, secretory units of islets in transplantation: an index for therapeutic management of islet transplanted patients and its application to type 2 diabetes. *Diabetes Res Clin Pract* 2006; 74: 222–226.
21. Japan Diabetes Society. Insulin treatment. In: Japan Diabetes Society (ed.). *Treatment Guide for Diabetes 2007*. Bunkodo, Japan, 2007; 47–55.
22. Franz MJ, Monk A, Barry B, *et al.* Effectiveness of medical nutrition therapy provided by dietitians in the management of non-insulin-dependent diabetes mellitus: a randomized, controlled clinical trial. *J Am Diet Assoc* 1995; 95: 1009–1017.
23. Ziemer DC, Berkowitz KJ, Panayioto RM, *et al.* A simple meal plan emphasizing healthy food choices is as effective as an exchange-based meal plan for urban African Americans with type 2 diabetes. *Diabetes Care* 2003; 26: 1719–1724.
24. Miller CK, Edwards L, Kissling G, *et al.* Nutrition education improves metabolic outcomes among older adults with diabetes mellitus: results from a randomized controlled trial. *Prev Med* 2002; 34: 252–259.
25. Japan Diabetes Society. Diet therapy. In: Japan Diabetes Society (ed.). *Treatment Guide for Diabetes 2007*. Bunkodo, Japan, 2007; 34–37.
26. Park SW, Ihm SH, Yoo HJ, *et al.* Differential effects of ambient blood glucose level and degree of obesity on basal serum C-peptide level and the C-peptide response to glucose and glucagon in non-insulin-dependent diabetes mellitus. *Diabetes Res Clin Pract* 1997; 37: 165–171.
27. Albareda M, Rigla M, Rodríguez-Espinosa J, *et al.* Influence of exogenous insulin on C-peptide levels in subjects with type 2 diabetes. *Diabetes Res Clin Pract* 2005; 68: 202–206.
28. Peacock I, Tattersall RB. The difficult choice of treatment for poorly controlled maturity onset diabetes: tablets or insulin? *Br Med J (Clin Res Ed)* 1984; 288: 1956–1959.
29. Sakuraba H, Mizukami H, Yagihashi N, *et al.* Reduced beta-cell mass and expression of oxidative stress-related DNA damage in the islet of Japanese Type II diabetic patients. *Diabetologia* 2002; 45: 85–96.
30. Butler AE, Janson J, Bonner-Weir S, *et al.* β-cell deficit and increased β-cell apoptosis in humans with type 2 diabetes. *Diabetes* 2003; 52: 102–110.
31. Rahier J, Guiot Y, Goebbels RM, *et al.* Pancreatic β-cell mass in European subjects with type 2 diabetes. *Diabetes Obes Metab* 2008; 10: 32–42.
32. Meier JJ, Menge BA, Breuer TG, *et al.* Functional assessment of pancreatic β-cell area in humans. *Diabetes* 2009; 58: 1595–1603.

SUPPORTING INFORMATION

Additional Supporting Information may be found in the online version of this article:

Figure S1 | Process of selection of subjects for analysis.
Figure S2 | Therapeutic modes of analyzed patients at admission and discharge, and the required alteration of therapy during the period of admission.
Figure S3 | Relative frequency distribution of C-peptide indices of patients with mean preprandial capillary plasma glucose levels of <130 mg/dL at discharge in the non-insulin and insulin group.
Table S1 | Details of medication and daily dosages of oral hypoglycemic agents used at discharge

Please note: Wiley-Blackwell are not responsible for the content or functionality of any supporting materials supplied by the authors. Any queries (other than missing material) should be directed to the corresponding author for the article.

ORIGINAL ARTICLE

Beneficial Effects of Exendin-4 on Experimental Polyneuropathy in Diabetic Mice

Tatsuhito Himeno,[1] Hideki Kamiya,[1,2] Keiko Naruse,[3] Norio Harada,[4] Nobuaki Ozaki,[1] Yusuke Seino,[1] Taiga Shibata,[1] Masaki Kondo,[1] Jiro Kato,[1] Tetsuji Okawa,[1] Ayako Fukami,[1] Yoji Hamada,[5] Nobuya Inagaki,[4] Yutaka Seino,[6] Daniel J. Drucker,[7] Yutaka Oiso,[1] and Jiro Nakamura[1]

OBJECTIVE—The therapeutic potential of exendin-4, an agonist of the glucagon-like peptide-1 receptor (GLP-1R), on diabetic polyneuropathy (DPN) in streptozotocin (STZ)-induced diabetic mice was investigated.

RESEARCH DESIGN AND METHODS—The presence of the GLP-1R in lumbar dorsal root ganglion (DRG) was evaluated by immunohistochemical analyses. DRG neurons were dissected from C57BL6/J mice and cultured with or without Schwann cell–conditioned media in the presence or absence of GLP-1 (7–37) or exendin-4. Then neurite outgrowth was determined. In animal-model experiments, mice were made diabetic by STZ administration, and after 12 weeks of diabetes, exendin-4 (10 nmol/kg) was intraperitoneally administered once daily for 4 weeks. Peripheral nerve function was determined by the current perception threshold and motor and sensory nerve conduction velocity (MNCV and SNCV, respectively). Sciatic nerve blood flow (SNBF) and intraepidermal nerve fiber densities (IENFDs) also were evaluated.

RESULTS—The expression of the GLP-1R in DRG neurons was confirmed. GLP-1 (7–37) and exendin-4 significantly promoted neurite outgrowth of DRG neurons. Both GLP-1R agonists accelerated the impaired neurite outgrowth of DRG neurons cultured with Schwann cell–conditioned media that mimicked the diabetic condition. At the doses used, exendin-4 had no effect on blood glucose or HbA_{1c} levels. Hypoalgesia and delayed MNCV and SNCV in diabetic mice were improved by exendin-4 without affecting the reduced SNBF. The decreased IENFDs in sole skins of diabetic mice were ameliorated by exendin-4.

CONCLUSIONS—Our findings indicate that exendin-4 ameliorates the severity of DPN, which may be achieved by its direct actions on DRG neurons and their axons. ***Diabetes* 60:2397–2406, 2011**

From the [1]Department of Endocrinology and Diabetes, Nagoya University Graduate School of Medicine, Nagoya, Japan; the [2]Department of Chronic Kidney Disease Initiatives, Nagoya University Graduate School of Medicine, Nagoya, Japan; the [3]Department of Internal Medicine, School of Dentistry, Aichi-Gakuin University, Nagoya, Japan; the [4]Department of Diabetes and Clinical Nutrition, Graduate School of Medicine, Kyoto University, Kyoto, Japan; the [5]Department of Metabolic Medicine, Nagoya University Graduate School of Medicine, Nagoya, Japan; the [6]Division of Diabetes, Clinical Nutrition, and Endocrinology, Department of Medicine, Kansai Electric Power Hospital, Osaka, Japan; and the [7]Department of Medicine, Mt. Sinai Hospital, Samuel Lunenfeld Research Institute, University of Toronto, Toronto, Ontario, Canada.

Corresponding author: Hideki Kamiya, hkamiya@med.nagoya-u.ac.jp.

Received 19 October 2010 and accepted 30 June 2011.

DOI: 10.2337/db10-1462

This article contains Supplementary Data online at http://diabetes.diabetesjournals.org/lookup/suppl/doi:10.2337/db10-1462/-/DC1.

Diabetes is the most common cause of peripheral neuropathy encompassing both mononeuropathy and polyneuropathy (1,2). In general, diabetic polyneuropathy (DPN) develops symmetrically in a nerve length–dependent fashion, with dying-back degeneration of both myelinated and unmyelinated fibers. Diabetic patients may exhibit various symptoms of DPN, such as spontaneous pain, hyperalgesia, and diminished sensation (3). It has been shown that tight glycemic control is effective in slowing the progression of DPN but cannot completely prevent it (4). We have focused on the role of reduced nerve blood flow in the development and the progression of DPN (5–7). In addition to the hemodynamic deterioration of diabetic nerves, previous studies have described a number of pathogenic mechanisms suggesting favorable treatments of DPN, but these treatments have generally failed in clinical trials (2). Thus, at this time, there are few effective therapies for DPN. Because the etiology of DPN seems to be multifactorial, a multitargeted intervention may be necessary.

An incretin hormone, glucagon-like peptide (GLP)-1, is released from the L cells of the small intestine (8). GLP-1 and a GLP-1 receptor (GLP-1R) agonist, exendin-4, potentiate glucose-stimulated insulin secretion after a meal, and GLP-1R agonists have been used as therapeutic agents for type 2 diabetes (9–11). In addition to this antihyperglycemic effect, GLP-1R agonists have been shown to have several actions, such as slowing gastric emptying (11) and reducing food intake (12), that are independent of insulin secretion (13). Many reports have suggested that GLP-1R agonists have neurotrophic and neuroprotective properties in some neurons and neural cells (14–18). It has been revealed that prolonged neurite extension is induced by mechanisms involving cAMP (19), which also is involved in the cascade mechanisms of insulin secretion induced by GLP-1R agonists. In addition, the therapeutic effects of GLP-1R agonists on stroke, Parkinsonism, and pyridoxine-induced peripheral sensory neuropathy (18–20) using animal models have been reported.

Although several beneficial effects of GLP-1 or the GLP-1R agonist on central and peripheral nervous systems have been reported, their effects under the diabetic condition have not yet been evaluated. Here, we investigated the effects of the GLP-1R agonist exendin-4 on DPN by both in vitro and in vivo experiments.

RESEARCH DESIGN AND METHODS

Schwann cell culture and preparation of Schwann cell–conditioned media. Immortalized Schwann cells (IMS32), established by long-term culture of adult mouse dorsal root ganglions (DRGs) and peripheral nerves (21), were a gift from Dr. Kazuhiro Watabe. IMS32 were cultured in Dulbecco's

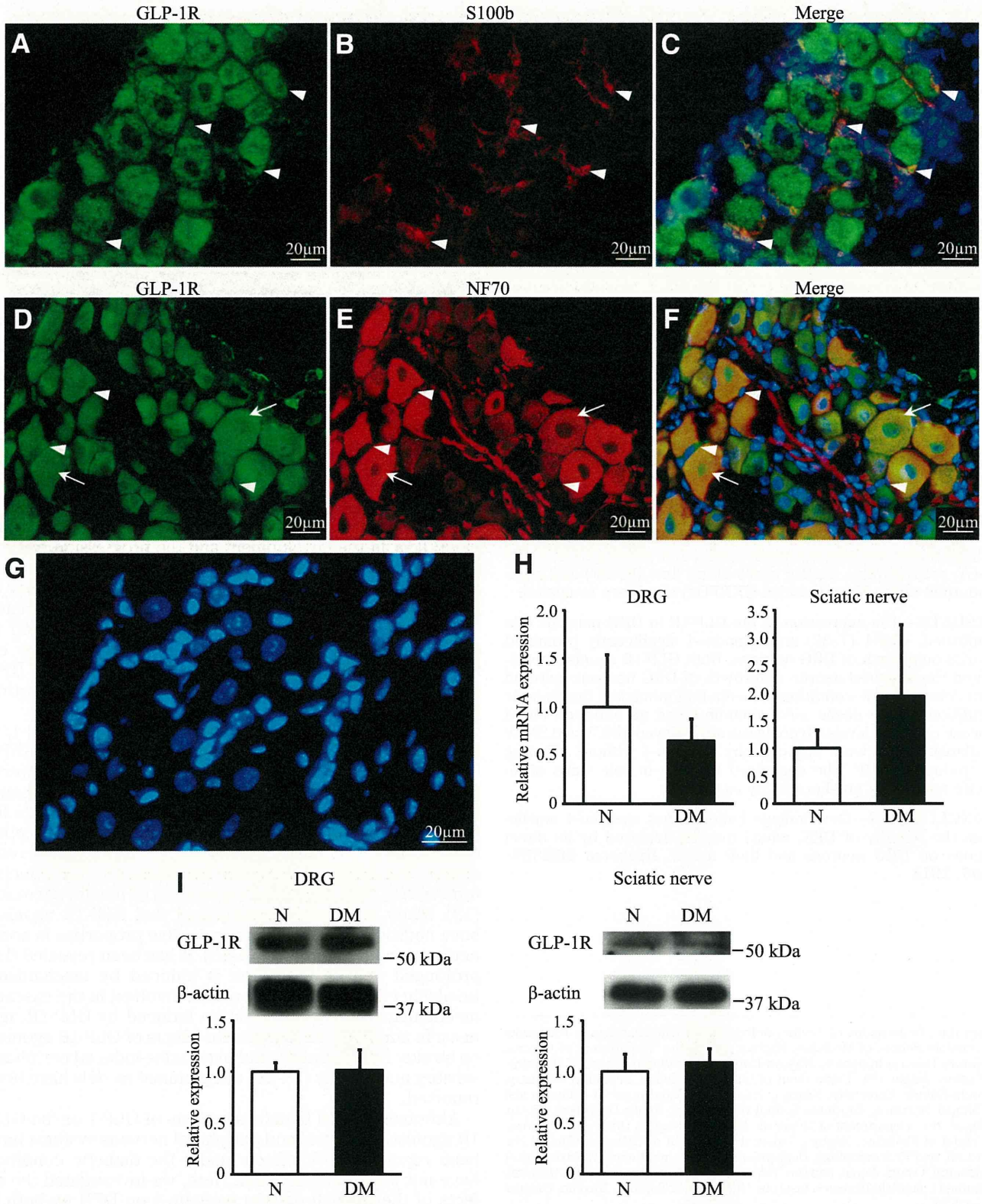

FIG. 1. Expression of GLP-1R in DRGs and sciatic nerves. *A*, *C*, *D*, and *F*: Immunohistochemically, GLP-1R (green) in DRG was detected with anti–GLP-1R antibody (sc-66911). Both DRG neurons, indicated by NF70 antibody (red) (*E* and *F*), and satellite glia cells, indicated by S100b antibody (red) (*B* and *C*), expressed GLP-1R. *C*, *F*, and *G*: Nuclei (blue) were stained with diaminido phenyl indol. *A–F*: White arrowheads indicate satellite glia cells. White arrows indicate neurons. *G*: GLP-1R protein (red) was not detected in DRG neurons of *glp1r*$^{-/-}$ mice. *H*: The transcript levels of *glp1r* in DRGs and sciatic nerves of diabetic mice were not significantly different from those of normal mice (DRG: normal mice [N] [n = 6], 1 ± 0.54, threshold cycle value [C_t] of *glp1r* 34.8 ± 2.3, C_t of 18S rRNA 11.2 ± 1.0 and diabetic mice [DM] [n = 7], 0.65 ± 0.23, C_t of *glp1r* 34.0 ± 1.5, C_t of 18S rRNA 11.0 ± 1.4, P = 0.544; sciatic nerves: normal mice [n = 4], 1 ± 0.34, C_t of *glp1r* 33.6 ± 1.6, C_t of 18S rRNA 14.7 ± 1.1 and diabetic mice [n = 5], 1.95 ± 1.29, C_t of *glp1r* 34.5 ± 1.3, C_t of 18S rRNA 12.5 ± 2.8, P = 0.606). *I*: There were no significant differences in the protein levels of GLP-1R

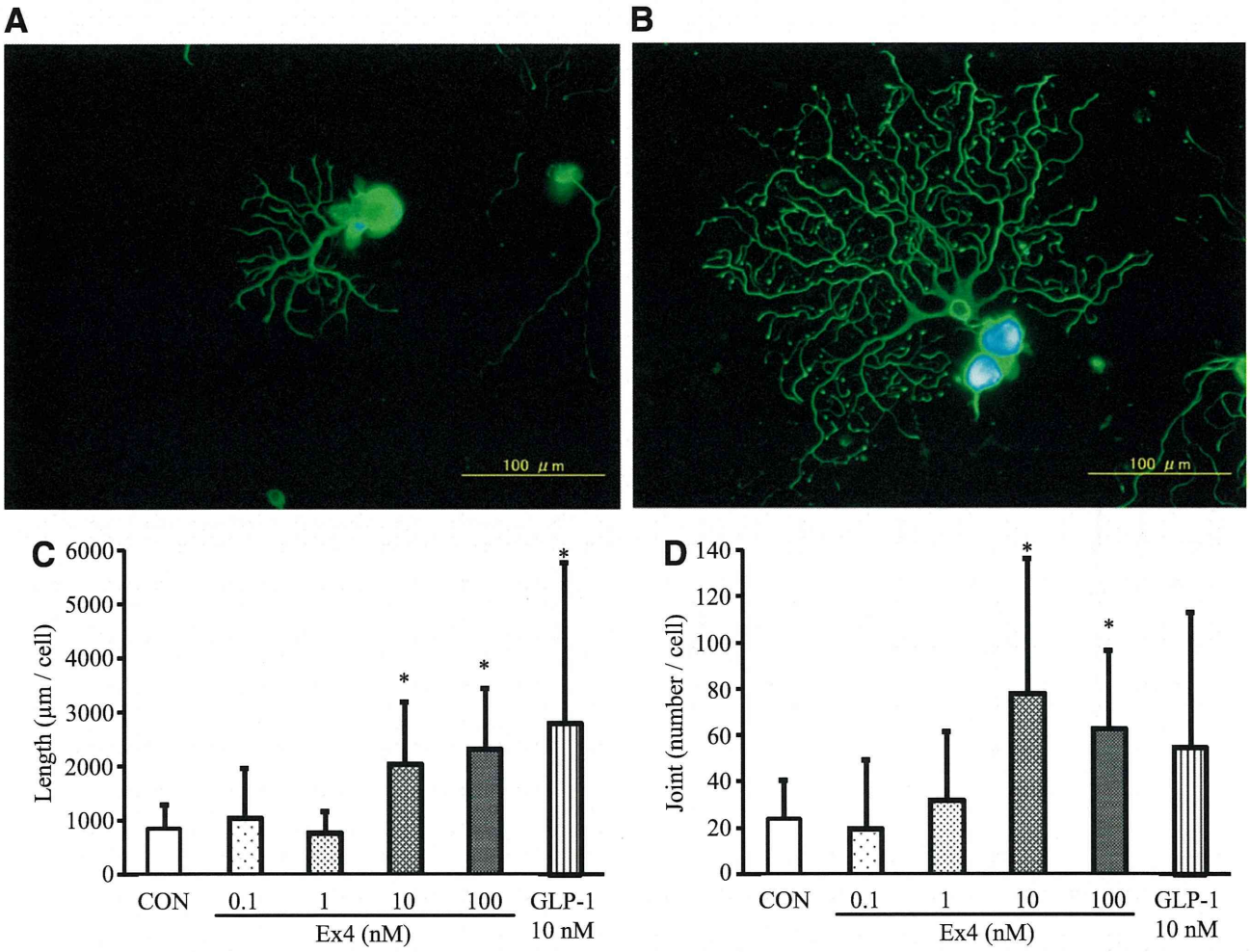

FIG. 2. Neurite outgrowth of DRG neurons by GLP-1 (7–37) and exendin-4 (Ex4). Representative fluorescence micrograph of DRG neurons cultured in the absence (*A*) or presence (*B*) of GLP-1 (7–37) (GLP-1) (10 nmol/L). GLP-1 (7–37) (10 nmol/L) or exendin-4 (0.1, 1, 10, and 100 nmol/L) increased the total neurite length (*C*) and joint number (*D*) of neurites. Results are means ± SD. CON, control medium. *$P < 0.05$ vs. control medium ($n = 10$–20). Control medium, joint number 23.5 ± 17.2 per cell, total length 833 ± 462 μm per cell, 10 nmol/L GLP-1 (7–37); joint number 54.8 ± 58.3, total length 2,786 ± 2,976, 0.1 nmol/L exendin-4; joint number 19.81 ± 29.59, total length 1,056.3 ± 904.5, 1 nmol/L exendin-4; joint number 32.23 ± 29.35, total length 761.9 ± 414.7, 10 nmol/L exendin-4; joint number 78.1 ± 58.4, total length 2,035 ± 1,162, 100 nmol/L exendin-4; and joint number 63.1 ± 33.8, total length 2,329 ± 1,104. (A high-quality digital representation of this figure is available in the online issue.)

modified Eagle's medium (DMEM) (Sigma-Aldrich, St. Louis, MO) containing 5.5 mmol/L D-glucose, penicillin (100 units/mL)-streptomycin (100 mg/mL), and 5% FBS (Moregate Biotech, Bulimba QLD, Australia). When the cells reached ~70% confluency, they were maintained in DMEM with 2% FBS containing 5.5 mmol/L D-glucose (normal glucose [NG]) or 30 mmol/L D-glucose (high glucose [HG]). After a 3-day culture, the cells were maintained in serum-free DMEM containing NG or HG. After 24 h, culture media were collected, concentrated 10 times using 10 kD centrifugal filters (Amicom Ultra-15; Nihon Millipore, Tokyo, Japan), and frozen at −80°C until use. We defined these media as NG-IMS media or HG-IMS media.

Primary culture of DRG neurons and evaluation of neurite outgrowth. DRG neuron cultures were prepared from 5-week-old male C57BL/6 mice (Chubu Kagaku Shizai, Nagoya, Japan), as previously described (22). In brief, DRGs were collected, dissociated by collagenase (Wako Pure Chemical, Osaka, Japan), and diluted in a medium consisting of F-12 media, 10 mmol/L glucose, and 30 nmol/L selenium. Isolated DRG neurons were seeded on glass coverslips coated with poly-L-lysine. DRG neurons were cultured with or without 10 nmol/L GLP-1 (7–37) (Bachem Bioscience, Torrance, CA) or exendin-4 (Sigma-Aldrich) (0.1, 1, 10, and 100 nmol/L). To evaluate the effects of GLP-1R agonists on impaired neurite outgrowth under the diabetic condition, DRG neurons were cultured in HG-IMS media that was diluted one-tenth with F-12 media.

After a 24-h culture, DRG neurons fixed with 4% paraformaldehyde were immunostained with rabbit polyclonal antineurofilament heavy-chain antibody (1:5,000; Nihon Millipore) and visualized with Alexa Fluor 488–coupled goat anti-rabbit IgG antibody (1:200; Invitrogen, Carlsbad, CA). Coverslips were counterstained with 4′,6-Diamidine-2′-phenylindole dihydrochloride (Merck, Tokyo, Japan). Images were captured by a charge-coupled device camera (DP70; Olympus Optical, Tokyo, Japan) using a fluorescence microscope (BX51; Olympus Optical). Neurite outgrowth was observed in 10–20 neurons per coverslip and evaluated by a computed image analysis system (Angiogenesis Image Analyzer version 2; KURABO Industries, Osaka, Japan).

Animals and induction of diabetes. Five-week-old male C57BL/6 mice (Chubu Kagaku Shizai) were used. Diabetes was induced by intraperitoneal injection of streptozotocin (STZ) (150 mg/kg; Sigma-Aldrich). Control mice received an equal volume of citric acid buffer. One week after STZ administration,

evaluated by Western blotting analyses between diabetic and normal mice (DRG: normal mice [$n = 4$], 1 ± 0.09 and diabetic mice [$n = 4$], 1.02 ± 0.20, $P = 0.875$; sciatic nerves: normal mice [$n = 4$], 1 ± 0.17 and diabetic mice [$n = 4$], 1.09 ± 1.35, $P = 0.438$). (A high-quality digital representation of this figure is available in the online issue.)

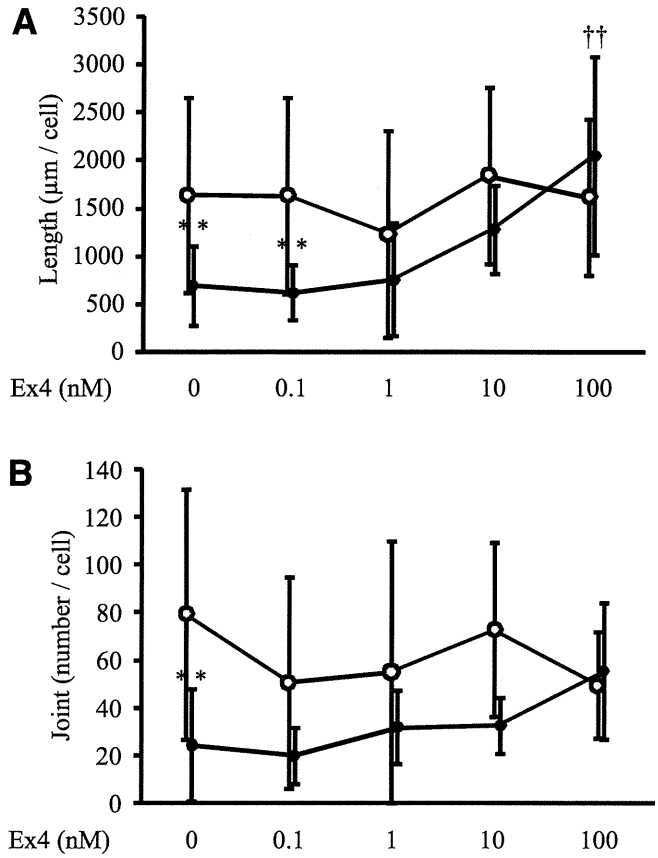

FIG. 3. Neurite outgrowth of DRG neurons in IMS media with or without exendin-4 (Ex4). Total length (*A*) and joint number (*B*) of DRG neurons cultured in IMS media were measured. Decreased total length and joint number of DRG neurites cultured in HG were ameliorated by Ex4 in a dose-dependent fashion. Results are means ± SD. ●, Neurite cultured in HG-IMS media; ○, neurite cultured in NG-IMS media. NG-IMS media were obtained from IMS cultured in F-12 media with 5.5 mmol/L D-glucose; HG-IMS media were obtained from IMS cultured in F-12 media with 30 mmol/L D-glucose. **$P < 0.005$ vs. NG-IMS media without exendin-4; ††$P < 0.005$ vs. HG-IMS media without exendin-4. n = 10–20. Total length: NG 1,635 ± 1,014 μm per cell and HG 684 ± 410; joint number: NG 79.2 ± 52.5 per cell and HG 24.2 ± 23.8. Total length: HG with 10 nmol/L exendin-4 1,278 ± 457 and HG with 100 nmol/L exendin-4 2,045 ± 1,029. Joint number: HG with 10 nmol/L exendin-4 32.3 ± 12.0 and HG with 100 nmol/L exendin-4 55.1 ± 28.8. Total length: NG with 10 nmol/L exendin-4 1,839 ± 915 and NG with 100 nmol/L exendin-4 1,614 ± 821. Joint number: NG with 10 nmol/L exendin-4 72.7 ± 36.3 and NG with 100 nmol/L exendin-4 49.3 ± 22.3.

the mice with plasma glucose concentrations >16 mmol/L were selected as diabetic mice. Twelve weeks after the induction of diabetes, mice were treated once daily with exendin-4 (10 nmol/kg in 0.1 mL of water i.p.) or vehicle (saline) over 4 weeks (n = 10 in each group). Before and after exendin-4 treatment, fasting blood glucose levels and HbA_{1c} were examined by a FreeStyle Freedom Glucose Meter (Nipro, Osaka, Japan) and a RAPIDIA Auto HbA1c-L assay kit using latex agglutination (Fujirebio, Tokyo, Japan), respectively. After the exendin-4 treatment, intraperitoneal glucose tolerance tests (IPGTTs) were performed on the mice. Serum insulin and glucagon levels also were measured in fasted mice by an insulin ELISA kit (Morinaga Institute of Biological Science, Yokohama, Japan) and a glucagon enzyme immune assay kit (Yanaihara Institute, Fujinomiya, Japan), respectively. The Nagoya University Institutional Animal Care and Use Committee approved the protocols of this experiment.

Measurement of current perception threshold using a neurometer. To determine a nociceptive threshold, the current perception threshold (CPT) was measured in 12- and 16-week diabetic and age-matched normal mice using a CPT/laboratory neurometer (Neurotron, Denver, CO). The electrodes (SRE-0405–8; Neurotron) for stimulation were attached to plantar surfaces. Each mouse was kept in a Ballman cage (Natsume Seisakusho, Tokyo, Japan) suitable for light restraint to keep awake. Three transcutaneous-sine-wave stimuli with different frequencies (2,000, 250, and 5 Hz) were applied to the plantar surfaces. The intensity of each stimulation was gradually increased automatically (increments of 0.01 mA for 5 and 250 Hz and increments of 0.02 mA for 2,000 Hz). The minimum intensity at which the mouse withdrew its paw was defined as the CPT. Six consecutive measurements were conducted at each frequency.

Nerve conduction velocity. Mice anesthetized with pentobarbital were placed on a heated pad in a room maintained at 25°C to ensure a constant rectal temperature of 37°C. Motor nerve conduction velocity (MNCV) was determined between the sciatic notch and ankle with a Neuropak NEM-3102 instrument (Nihon-Koden, Osaka, Japan), as previously described (5,6,23). The sensory nerve conduction velocity (SNCV) was measured between the knee and ankle with retrograde stimulation.

Sciatic nerve blood flow. Sciatic nerve blood flow (SNBF) was measured by laser-Doppler flowmetry (FLO-N1; Omegawave, Tokyo, Japan). The thigh skin of an anesthetized mouse was cut along the femur and then an incision through the fascia was carefully made to expose the sciatic nerve. Five minutes after this procedure, the blood flow was measured by a laser-Doppler probe placed 1 mm above the nerve. During this measurement, the mouse was placed on a heated pad in a room maintained at 25°C to ensure a constant rectal temperature of 37°C.

Tissue collection. Four weeks after the treatment with exendin-4, mice were killed by an overdose of pentobarbital or perfusion with 50 mL of 4% paraformaldehyde. DRGs and sciatic nerves were obtained from normal and diabetic mice. Some of the tissues were snap frozen in liquid nitrogen, followed by preservation at –80°C until use, and others were transferred to RNAlater solution (Invitrogen), followed by freezing preservation for RT-PCR. For immunohistochemistry, DRGs, pancreas, and sole skin were excised, fixed in 4% paraformaldehyde, and frozen in optimal cutting temperature compound (Sakura Finetechnical, Tokyo, Japan) after cryoprotection.

GLP-1R mRNA expression in DRGs and sciatic nerves. RNAs were extracted from frozen samples of DRGs and sciatic nerves using Isogen (Nippon Gene, Toyama, Japan) and were quantified spectrophotometrically. Starting from 1 μg of RNA, cDNA was synthesized using ReverTra Ace (Toyobo, Osaka, Japan). TaqMan gene expression assays (Applied Biosystems, Foster City, CA) were used for GLP-1R and 18S rRNA for the endogenous control. Real-time quantitative RT-PCR was performed using the Mx3000P QPCR System (Stratagene, La Jolla, CA). Relative quantity was calculated by the $\Delta\Delta C_t$ method with normalization to 18S rRNA (24).

Western blotting. DRGs and sciatic nerves were used for Western blotting. Samples were lysed in detergent lysis buffer (Cell Lysis Buffer; Cell Signaling Technology, Boston, MA) adding 1 mmol/L phenylmethanesulfonylfluoride (Sigma-Aldrich), following centrifugation. Proteins were quantitated the concentrations with a bicinchoninic acid assay (Sigma Chemical) and were transferred to polyvinylidene fluoride membranes (Millipore, Billerica, MA) after SDS-PAGE. Membranes were blocked and incubated with rabbit polyclonal anti–GLP-1R antibody (1:100; Santa Cruz Biotechnology, Santa Cruz, CA) and rabbit polyclonal anti–β-actin antibody (1:10,000; Abcam, Cambridge, MA). Antigen detection was performed using ECL Plus Western Blotting Detection Reagents (Amersham Pharmacia Biotech, Piscataway, NJ) with horseradish peroxidase–conjugated anti-rabbit IgG antibody (1:6,000; Cell Signaling Technology). Images were scanned and their densities were determined by ImageJ (National Institutes of Health, Bethesda, MD). The expression of the GLP-1R protein was corrected by β-actin density, and the expression in tissues of normal mice was arbitrarily set at 1.0.

Immunocytochemistry and frozen section staining. After a 24-h culture, DRG cells, as indicated above, were fixed with 4% paraformaldehyde. The cells were blocked with 3% goat serum, and the following primary antibodies were applied to the glass coverslips at 4°C overnight: rabbit polyclonal anti–GLP-1R antibody (1:200, sc-66911; Santa Cruz Biotechnology); mouse monoclonal anti-neurofilament 70 kDa (NF70) antibody (1:1,000, MAB1615; Millipore); and mouse monoclonal anti-S100b antibody (1:300, S2532; Sigma-Aldrich). After washing, the following secondary antibodies were loaded for 1 h at room temperature in a dark box: Alexa Fluor 488–coupled goat anti-rabbit IgG antibody (1:200; Invitrogen) and Alexa Fluor 594–coupled goat anti-mouse antibody (1:300; Invitrogen).

For immunohistochemistry, after the microwave irradiation in citrate buffer (pH 6.0), cryostat sections were blocked with 5% skim milk (Meiji Milk, Tokyo, Japan) and the following primary antibodies were applied to the sections at 4°C overnight: rabbit polyclonal anti–protein-gene-product 9.5 (PGP 9.5) antibody (1:500; Millipore); guinea-pig polyclonal anti-insulin antibody (1:500, Ab7842-500; Abcam); rabbit polyclonal anti–GLP-1R antibody (1:200, sc-66911, Santa Cruz Biotechnology; LS-A1205 and LS-A1206, MBL International, Woburn, MA); mouse monoclonal NF70 antibody (1:1,000; Millipore); and mouse monoclonal anti-S100b antibody (1:300; Sigma-Aldrich). After washing, the secondary antibodies, as indicated above, were loaded for 1 h at room temperature.

TABLE 1
Body weight, blood glucose, and HbA_{1c} levels in normal and diabetic mice

	Normal mice			Diabetic mice		
		Posttreatment			Posttreatment	
	Pretreatment	Saline	Exendin-4	Pretreatment	Saline	Exendin-4
n	8	5	6–8	9–10	8	9
Blood glucose (mmol/L)	9.1 ± 1.6	9.1 ± 1.6	8.7 ± 2.4	23.1 ± 2.8*	26.6 ± 2.9*	23.9 ± 2.3*
HbA_{1c} (%)	4.0 ± 0.1	4.1 ± 0.2	3.9 ± 0.1	7.6 ± 1.2*	7.7 ± 2.1*	6.9 ± 2.1*
Body weight (g)	31 ± 3	31 ± 3	27 ± 2†	26 ± 3*	24 ± 4*	23 ± 2*

Data are means ± SD. *$P < 0.05$ vs. pretreatment normal mice. †$P < 0.05$ vs. normal mice treated with saline.

Coverslips and tissues were counterstained with diaminido phenyl indol (Merck). Images were captured by a charge-coupled device camera (DP70; Olympus Optical) using a fluorescence microscope (BX51; Olympus Optical).

Measurement of intraepidermal nerve fiber densities. Nerve fibers stained with anti–PGP 9.5 antibody were counted as previously reported (25). In brief, each individual nerve fiber with branching inside the epidermis was counted as one, and a nerve fiber with branching in the dermis was counted separately. Six fields from each section were randomly selected for the intraepidermal nerve fiber (IENF) densities (IENFDs). IENFDs were derived and expressed as epidermal nerve fiber numbers per length of the epidermal basement membrane (fibers per millimeter).

Statistical analysis. All the group values were expressed as means ± SD. Statistical analyses were made by one-way ANOVA, with the Bonferroni correction for multiple comparisons. All analyses were performed by personnel who were unaware of the animal identities.

RESULTS

DRG neurons and satellite cells expressed GLP-1Rs. To confirm the quality of GLP-1R antibody, we stained the islets of *glp1r*$^{-/-}$ mice. GLP-1R antibody obtained from Santa Cruz (sc-66911) detected the β-cells of wild-type mice but not those of *glp1r*$^{-/-}$ mice. In contrast, GLP-1R antibodies from MBL International (LS-A1205 and LS-A1206) nonspecifically stained the islets of *glp1r*$^{-/-}$ mice (Supplementary Fig. 1). In addition to immunohistochemistry, GLP-1R protein in the pancreas of wild-type mice was specifically detected and that of *glp1r*$^{-/-}$ mice was undetected with the GLP-1R antibody from Santa Cruz by Western blotting methods (Supplementary Fig. 2). Therefore, in this study, we used sc-66911 as a primary antibody to detect the expression of GLP-1R in DRGs. GLP-1R expression was detected in both DRG neurons indicated by NF70 and satellite cells indicated by S100b antibody (Fig. 1*A–F*). In contrast to these wild-type mice DRGs, GLP-1R expression was not detected in the DRGs of *glp1r*$^{-/-}$ mice (Fig. 1*G*). To further evaluate the localization of GLP-1R, we stained enzymatically dissociated DRG cells with GLP-1R antibody in addition to S100b or NF70 antibody. GLP-1R proteins also were expressed in both DRG neurons and satellite cells by this immucytochemical method (Supplementary Fig. 3).

GLP-1R agonists promoted neurite outgrowth of DRG neurons. In our DRG culture system, GLP-1R protein was expressed in all neurons and in about two-thirds of glia cells (data not shown). Therefore, we used our DRG culture system to evaluate the impact of the GLP-1R agonist on the sensory nervous system, especially sensory neurons.

Neurite outgrowth of DRG neurons was increased in the presence of GLP-1 (7–37) or exendin-4 (Fig. 2*A* and *B*). Total length and joint number of neurites were significantly increased by GLP-1 (7–37) or exendin-4 (joint number: control vs. 10 nmol/L exendin-4, $P = 0.0002$; control vs. 100 nmol/L exendin-4, $P = 0.0093$; and control vs. 10 nmol/L GLP-1 (7–37), $P < 0.0001$; total length: control vs. 10 nmol/L exendin-4, $P = 0.0003$; control vs. 100 nmol/L exendin-4, $P < 0.0001$; and control vs. 10 nmol/L GLP-1 (7–37), $P < 0.0001$) (Fig. 2*C* and *D*).

Exendin-4 ameliorated high glucose–induced reduction in neurite outgrowth of DRG neurons. DRG neurons cultured with HG-IMS media, which mimicked the diabetic state, had shorter neurites and smaller joint numbers compared with those cultured with NG-IMS media, which mimicked the nondiabetic normal state (total length: $P = 0.0205$, joint number: $P = 0.0006$) (Fig. 3). The impaired neurite outgrowth of DRG neurons cultured with HG-IMS media was improved by exendin-4 (total length: HG with 10 nmol/L exendin-4, $P = 0.1620$, and HG with 100 nmol/L exendin-4, $P = 0.0012$; joint number: HG with 10 nmol/L exendin-4, $P = 0.5871$, and HG with 100 nmol/L exendin-4, $P = 0.0433$). In contrast, exendin-4 did not promote the neurite outgrowth of DRG neurons cultured with NG-IMS media.

Levels of GLP-1R in DRGs and sciatic nerves were not impaired in diabetic mice. To ascertain the levels of *glp1r* mRNA and protein, we carried out real-time PCR analyses and Western blotting analyses in the DRGs and sciatic nerves of normal and diabetic mice before the exendin-4 treatment. The levels of *glp1r* transcript in DRGs and sciatic nerves of diabetic mice were not significantly different between those of normal mice (DRG: $P = 0.544$, sciatic nerves: $P = 0.606$) (Fig. 1*H*). Furthermore, there were no significant differences in GLP-1R protein contents between diabetic and normal mice (DRG: $P = 0.875$, sciatic nerves: $P = 0.438$) (Fig. 1*I*).

Body weights, blood glucose levels, and HbA_{1c}. At 12 weeks, diabetic mice showed severe hyperglycemia ($P = 0.0003$) and significantly reduced body weight gain ($P = 0.003$). Random blood glucose levels measured during the experimental period were not significantly different in any group. Exendin-4 treatment for 4 weeks did not alter body weight, blood glucose, or HbA_{1c} levels in the diabetic groups (Table 1).

Serum insulin and glucagon levels and IPGTTs. After the exendin-4 treatment, serum insulin levels were significantly decreased in diabetic mice, and exendin-4 administration provided no significant improvement in both diabetic and normal mice (Supplementary Fig. 4*A*). In IPGTT, blood glucose levels in diabetic mice after 15 min of glucose injection were significantly elevated compared with those in normal mice. These elevations were not significantly decreased by exendin-4 treatment (Supplementary Fig. 4*C*).

Although serum glucagon concentrations were not incremented in diabetic mice compared with those in normal mice, the concentrations in diabetic mice had a high propensity to be decreased by exendin-4 treatment (Supplementary Fig. 4*B*).

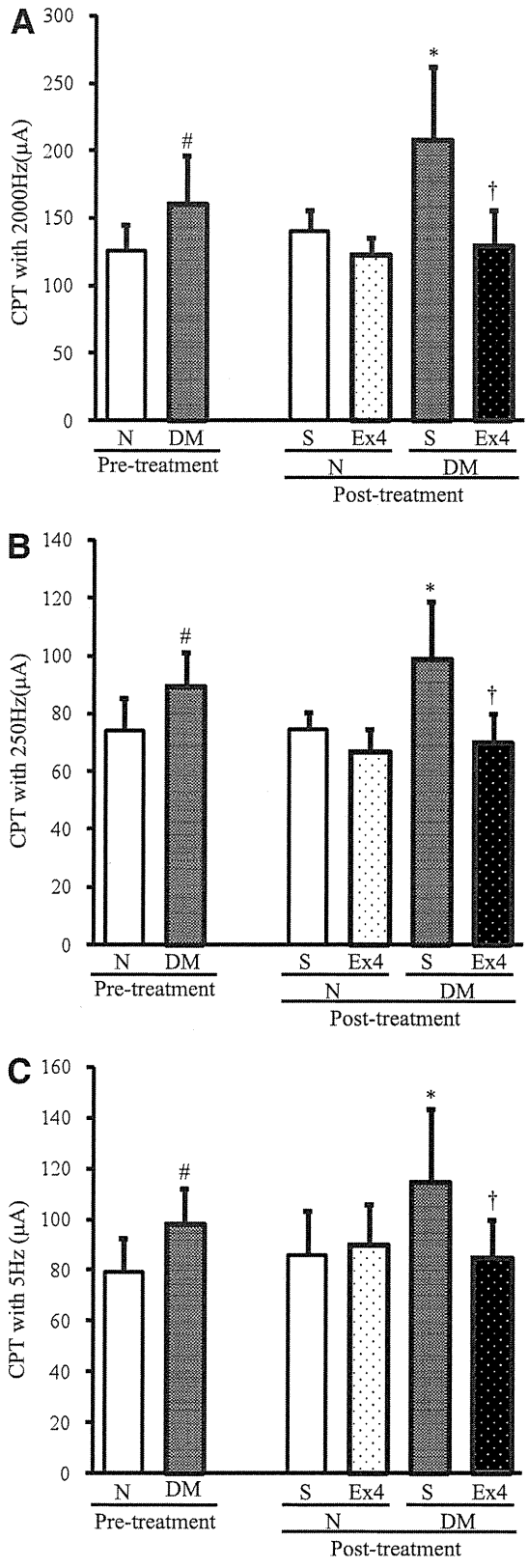

FIG. 4. Evaluation of sensory nerve functions. Measurements of CPTs at 2,000 (*A*), 250 (*B*), and 5 (*C*) Hz by a neurometer were performed before and at the end of exendin-4 (Ex4) administration. CPTs for all pulses were significantly increased in the diabetic group (DM), and these deficits were significantly prevented by exendin-4. N, normal mice; S, saline. Results are means ± SD. #P < 0.05 vs. pretreatment normal mice; *P < 0.05 vs. saline-treated normal mice; †P < 0.05 vs. saline-treated diabetic mice. Saline-treated normal mice, n = 8; exendin-4–treated normal mice, n = 8; saline-treated diabetic mice, n = 9; exendin-4–treated diabetic mice, n = 9.

Reduced sensory perception in diabetic mice was ameliorated by exendin-4 administration. After 12 weeks of diabetes, CPTs at 5, 250, and 2,000 Hz were significantly increased compared with those in normal mice (5 Hz: P = 0.015, 250 Hz: P = 0.019, and 2,000 Hz: P = 0.028), representing hypoalgesia in diabetic mice. After the 4 weeks of exendin-4 administration, these deficits in sensation were significantly improved in diabetic mice compared with saline-treated diabetic controls (5 Hz: P = 0.0161, 250 Hz: P = 0.0012, and 2,000 Hz: P = 0.0011). The injection of exendin-4 into normal mice did not induce significant changes in CPTs (Fig. 4*A–C*).

Exendin-4 improved delayed NCVs in diabetic mice. MNCVs and SNCVs of diabetic mice were significantly delayed compared with those of normal mice (MNCV: P = 0.0341, SNCV: P = 0.0489). The delay in MNCVs and SNCVs was significantly restored by exendin-4 treatment (MNCV: P = 0.0289, SNCV: P = 0.0201) (Fig. 5*A* and *B*). However, exendin-4 administration did not alter NCVs in normal mice.

Nerve fibers in epidermis were preserved by exendin-4. IENFDs were evident in both the epidermis and the dermis of the foot skin by the fluorescent imaging (Fig. 6*A*). Although IENFDs were decreased in diabetic mice (P = 0.0011), this decrement was significantly ameliorated by exendin-4 (P = 0.0007) (Fig. 6*B*). Administration of exendin-4 did not change IENFDs in normal mice (P = 0.2212).

Exendin-4 had no effects on SNBF. SNBF in diabetic mice was significantly decreased compared with those in normal mice (P = 0.0203), and the decrease was not ameliorated by exendin-4 (P = 0.7407) (Fig. 7).

DISCUSSION

In this study, we investigated whether GLP-1R agonists have therapeutic effects on DPN. First, we confirmed the expression of the GLP-1R on DRG neurons by immunohistochemical analyses. Second, we observed that both GLP-1 (7–37) and exendin-4 promoted neurite outgrowth of DRG neurons, and exendin-4 ameliorated the impaired neurite outgrowth of DRG neurons in conditioned media obtained from Schwann cell cultures under high-glucose conditions. We then demonstrated that administration of exendin-4 improved the reduced sensory perception of the plantar pedis, delayed NCVs of hindlimbs, and decreased IENFDs of the plantar skin in diabetic mice. However, neither the hyperglycemic state nor decreased SNBF were improved by exendin-4. These results indicate that exendin-4 has direct effects on peripheral nerves that are independent of its antihyperglycemic and hemodynamic effects.

Several antibodies against the GLP-1R are commercially available. GLP-1R antibodies, LS-A1205 and LS-A1206, produced by MBL International, have recently been used in some studies (26–28). To confirm the reliability of these antibodies, we stained islet cells in which the presence of the GLP-1R has repeatedly been demonstrated (29,30). LS-A1205 and LS-A1206 distinctively reacted with β-cells that also were clearly stained with anti-insulin antibody, but these antisera also reacted with β-cells or perhaps α-cells in $Glp1r^{-/-}$ mice. We then tested another antibody for GLP-1R, sc-66911 (Santa Cruz). This antiserum detected β-cells

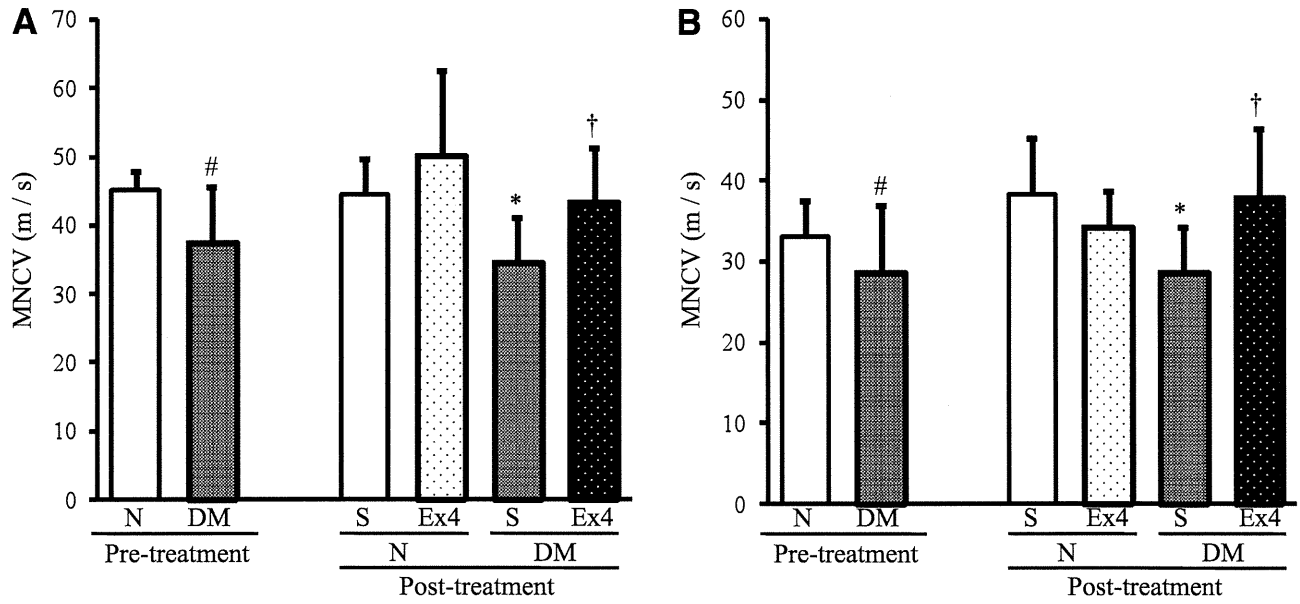

FIG. 5. NCVs. MNCV (*A*) and SNCV (*B*) were measured before and after the treatment with exendin-4 (Ex4). DM, diabetic mice; N, normal mice; S, saline. Before the treatment: MNCV for normal mice 45.2 ± 2.7 m/s and diabetic mice 37.5 ± 8.2, $P = 0.0341$; SNCV for normal mice 33.0 ± 4.6 and diabetic mice 28.6 ± 7.2, $P = 0.0489$. After the treatment: MNCV for saline-treated diabetic mice 34.5 ± 8.1 and exendin-4–treated diabetic mice 43.3 ± 7.9, $P = 0.0289$; SNCV for saline-treated diabetic mice 28.6 ± 5.6 and exendin-4–treated diabetic mice 38.0 ± 8.5, $P = 0.0201$. Results are means ± SD. #$P < 0.05$ vs. pretreatment normal mice. *$P < 0.05$ vs. saline-treated normal mice. †$P < 0.05$ vs. saline-treated diabetic mice. Saline-treated normal mice, $n = 7$; exendin-4–treated normal mice, $n = 8$; saline-treated diabetic mice, $n = 8$; exendin-4–treated diabetic mice, $n = 8$.

of wild-type mice but did not react with those of *glp1r*$^{-/-}$ mice (Supplementary Fig. 1). Furthermore, the antiserum detected GLP-1R proteins in the pancreata of wild-type mice but not in that of *glp1r*$^{-/-}$ mice, using immunoblotting assay. We confirmed the expression of GLP-1R in DRG neurons and glia cells with a GLP-1R antibody, sc-66911.

GLP-1 and exendin-4 previously have been shown to promote neurite outgrowth of rat pheochromocytoma cells (19,31) and to protect rat primary hippocampal neurons from cell death (14). It has been reported that exogenous GLP-1R activation significantly reduces glucose-dependent reactive oxygen species generation in hypothalamus (32). These antioxidative effects of GLP-1R agonists might yield benefits to central and peripheral nervous systems.

The dipeptidyl peptidase (DPP)-IV inhibitor (vildagliptin) recently has been shown to prevent peripheral nerve degeneration in STZ-induced diabetic mice (33). Although GLP-1 is one of the substrates of DPP-IV, several bioactive peptides, such as neuropeptide Y, substance P, glucagon-like peptide-2, and stromal cell–derived factor-1α also have been reported as substrates of DPP-IV (34,35). Among these peptides, neuropeptide Y and substance P are known as neurotransmitters or modulators of peripheral nervous systems (36,37), and it also has been demonstrated that stromal cell–derived factor-1α released from DRG glia regulates leukocyte chemotaxis and modulates neuropathic pain behavior (38). Therefore, the preventive effects of the DPP-IV inhibitor on DPN may be attributed to its protective effects on these neurotrophic peptides and mediated through increased levels of GLP-1.

Although we cannot infer the precise site(s) of action of exendin-4 in our diabetic mice that ameliorated DPN in vivo, our data using cellular models of DPN in vitro implicate a direct role for GLP-1 and the GLP-1R agonist exendin-4. We previously reported that conditioned media obtained from Schwann cell cultures under high-glucose conditions impaired neurite outgrowth of DRG neurons, likely mediated through a decrease in nerve growth factor production (21). In our current study, the impaired neurite outgrowth induced by hyperglycemia-conditioned IMS media was improved by exendin-4. In contrast, under the normal glucose–conditioned IMS media, which mimicked the nondiabetic normal state, exendin-4 did not exert any changes in neurite outgrowth because of basal enhancement of neurite outgrowth by various growth factors, such as nerve growth factor secreted from Schwann cells (21). These results indicate that GLP-1R agonists exert regenerative effects on peripheral sensory neurons under experimental conditions, mimicking diabetes in vitro. Additional studies on the effect on the role of downstream neurotrophic factors, such as nerve growth factor, will be required to evaluate the mechanism of action of GLP-1R agonists.

We also demonstrated the effects of exendin-4 on DPN in STZ-induced diabetic mice. We evaluated sensory nerve functions using a CPT/laboratory neurometer. The neurometer is now widely and clinically used to evaluate the effects of analgesic drugs and peripheral nerve functions in various painful neuropathies, including DPN (39–42). In this study, after 12 weeks of diabetes, hypoalgesia at 2,000, 250, and 5 Hz was observed in the diabetic mice, and injection of exendin-4 improved these abnormalities. In addition, exendin-4 ameliorated the decreased IENFDs in diabetic mice. The restoration of sensory functions by exendin-4 was confirmed by the improvement of IENFDs.

In addition, we measured MNCVs and SNCVs that represent relatively large axonal functions. Both the delayed MNCVs and SNCVs in diabetic mice were improved by exendin-4, indicating that exendin-4 had therapeutic effects on impaired motor and sensory nerve functions. These data also are consistent with previous reports (14,16,18,19) that revealed the plausible effects of GLP-1 or GLP-1R agonists on central and peripheral nerve disorders.

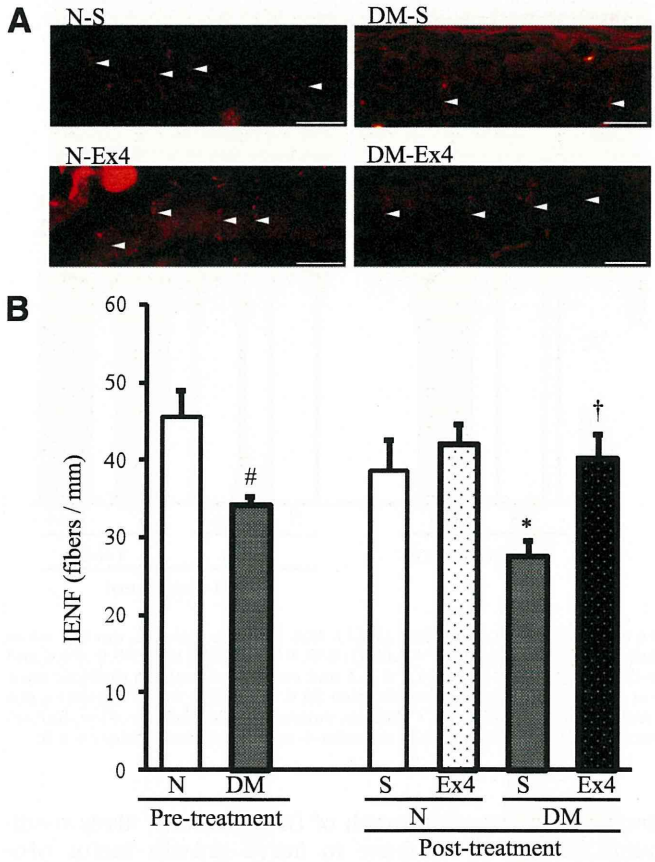

FIG. 6. IENFDs after the treatment with exendin-4 (Ex4). *A*: IENFs indicated by white arrowheads were detected by immunofluorescence assay with anti–PGP 9.5 antibody (red). *B*: Quantification of the density revealed a significant decrement in untreated diabetic mice and the significant amelioration by exendin-4 treatment. DM, diabetic mice; N, normal mice; S, saline. Bar: 20 μm. Saline-treated normal mice 38.5 ± 3.9, saline-treated diabetic mice 27.7 ± 1.9, exendin-4–treated normal mice 42.1 ± 2.4, and exendin-4–treated diabetic mice 40.2 ± 3.1 fibers per mm. Results are means ± SD. #$P < 0.05$ vs. pretreatment normal mice. *$P < 0.05$ vs. saline-treated normal mice. †$P < 0.05$ vs. saline-treated diabetic mice. Saline-treated normal mice, $n = 4$; exendin-4–treated normal mice, $n = 3$; saline-treated diabetic mice, $n = 4$; exendin-4–treated diabetic mice, $n = 3$. (A high-quality digital representation of this figure is available in the online issue.)

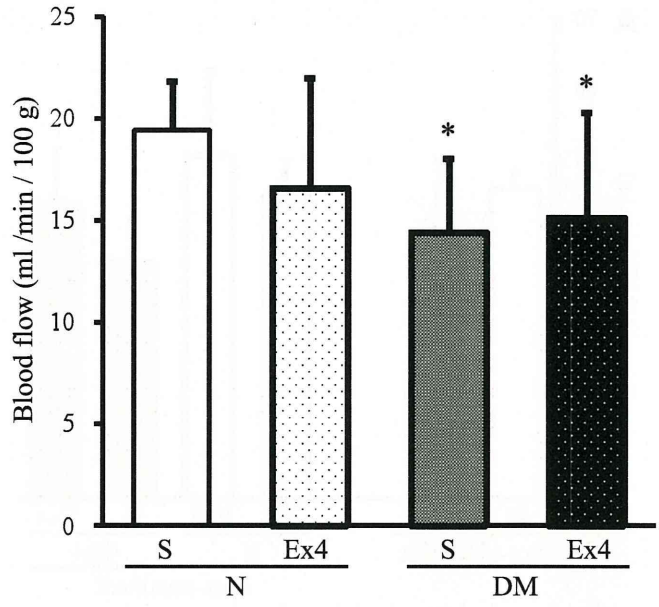

FIG. 7. SNBF treated with or without exendin-4 (Ex4) in normal (N) or diabetic (DM) mice. S, saline. Saline-treated normal mice 19.4 ± 2.4, saline-treated diabetic mice 14.4 ± 3.6, and exendin-4–treated diabetic mice 15.2 ± 5.2 mL/min/100 g. Results are means ± SD. *$P < 0.05$ vs. saline-treated normal mice. Saline-treated normal mice, $n = 9$; exendin-4–treated normal mice, $n = 8$; saline-treated diabetic mice, $n = 8$; exendin-4–treated diabetic mice, $n = 9$.

Decreased nerve blood flow has been recognized as one of the most important mechanisms in the development of DPN. Recently, GLP-1R has been detected in blood vessels, and the beneficial effects of GLP-1 or GLP-1R agonists on vascular functions have been reported (28,43,44). In our experimental study, however, exendin-4 did not alter normal nerve blood flow in normal mice nor did it improve the reduced nerve blood flow in diabetic mice. One of the reasons for this discrepancy is that the vasodilatory actions of GLP-1 agonists are likely mediated mainly through a GLP-1R–independent pathway, which depends on a GLP-1 metabolite, GLP-1 (9–36) (28). In our present study, therefore, exendin-4 could not exert vasoregulatory effects. Another reason is that the central-peripheral sympathetic nervous system function would likely be impaired in the diabetic state. It has been reported that GLP-1 in the central nervous system regulates sympathetic outflow, resulting in increases in blood pressure and heart rate independent of the peripheral actions of GLP-1 on glucoregulation (43,44). As mice with a long duration of diabetes in the current study might have developed sympathetic nerve dysfunction, exendin-4 may have been unable to modulate nerve blood flow after prolonged experimental diabetes. Although the precise mechanisms remain unclear, the effects of exendin-4 on DPN may be attributed to its direct actions on DRG neurons and their axons.

Because GLP-1R agonists possess glucose-lowering effects, we used a dosing regimen that did not produce sustained reductions in blood glucose or body weight. Although trends toward reduced levels of HbA_{1c} and glucagon were observed in exendin-4–treated diabetic mice (Table 1 and Supplementary Fig. 4), there were no significant differences in the glucose levels, insulin concentrations, or IPGTTs between exendin-4–treated and untreated mice. In previous studies (45,46), exendin-4 was administrated at the same time as or before STZ injection. On the other hand, we started exendin-4 injections 12 weeks after the onset of diabetes. Because HbA_{1c} in diabetic mice treated with exendin-4 tended to decrease (Table 1), longer treatment or larger doses of exendin-4 might have significantly improved hyperglycemia, indirectly contributing to the amelioration of DPN. In the current study, however, it is conceivable that the effectiveness of exendin-4 on DPN may be independent of the glucose-lowering effects.

Miki et al. (47) previously reported that glucose-responsive neurons in the hypothalamus regulate the secretion of glucagon and govern the glucose homeostasis. In addition, it was shown in a recent study that GLP-1R agonists had a glucagon-lowering effect (48), which is consistent with the present observation that glucagon concentrations tended to be decreased by the administration of exendin-4 in diabetic mice. It remains to be evaluated whether the glucagon levels influence the pathophysiology of DPN through mechanisms independent of hyperglycemia.

In conclusion, we demonstrated the beneficial effects of GLP-1R agonist on DPN. GLP-1 analogs and GLP-1R

agonists have been broadly used as antihyperglycemic agents in type 2 diabetic patients. In addition to the established use of these agents to control blood glucose, there currently is little data demonstrating an effect of GLP-1R agonists on peripheral nerve functions. Our data demonstrating the improvement of experimental DPN after administration of GLP-1 and exendin-4 suggest that additional clinical investigation with attention to whether therapy with GLP-1R agonists produce changes in DPN may be warranted.

ACKNOWLEDGMENTS

This research was supported in part by a grant-in-aid for scientific research (21592506) from the Ministry of Education, Culture, Sports, Science, and Technology (MEXT) and in part by the "Strategic Research AGU-Platform Formation (2008–2012)" Project for Private Universities: matching fund subsidy from MEXT of Japan.

No potential conflicts of interest relevant to this article were reported.

T.H. researched data. H.K. designed the animal and cell culture studies and contributed to the writing and editing of the manuscript. K.N. contributed to discussion. N.H. was responsible for the maintenance of the animals. N.O. and Yus.S. contributed to discussion. T.S. and M.K. reviewed the manuscript. J.K., T.O., and A.F. researched data. Y.H. contributed to discussion. N.I. was responsible for the maintenance of the animals. Yut.S. and D.J.D. wrote, reviewed, and edited the manuscript. Y.O. contributed to discussion. J.N. wrote, reviewed, and edited the manuscript.

The authors thank Michiko Yamada, Keiko Shimamoto, Naoko Furukawa, Chikako Nagase, and Mayumi Katagiri, from the Department of Endocrinology and Diabetes, Nagoya University Graduate School of Medicine, for technical assistance.

REFERENCES

1. Toth C, Brussee V, Cheng C, Zochodne DW. Diabetes mellitus and the sensory neuron. J Neuropathol Exp Neurol 2004;63:561–573
2. Zochodne DW. Diabetes mellitus and the peripheral nervous system: manifestations and mechanisms. Muscle Nerve 2007;36:144–166
3. Kles KA, Vinik AI. Pathophysiology and treatment of diabetic peripheral neuropathy: the case for diabetic neurovascular function as an essential component. Curr Diabetes Rev 2006;2:131–145
4. Genuth S. Insights from the diabetes control and complications trial/epidemiology of diabetes interventions and complications study on the use of intensive glycemic treatment to reduce the risk of complications of type 1 diabetes. Endocr Pract 2006;12(Suppl. 1):34–41
5. Nakae M, Kamiya H, Naruse K, et al. Effects of basic fibroblast growth factor on experimental diabetic neuropathy in rats. Diabetes 2006;55:1470–1477
6. Naruse K, Hamada Y, Nakashima E, et al. Therapeutic neovascularization using cord blood-derived endothelial progenitor cells for diabetic neuropathy. Diabetes 2005;54:1823–1828
7. Shibata T, Naruse K, Kamiya H, et al. Transplantation of bone marrow-derived mesenchymal stem cells improves diabetic polyneuropathy in rats. Diabetes 2008;57:3099–3107
8. Drucker DJ, Nauck MA. The incretin system: glucagon-like peptide-1 receptor agonists and dipeptidyl peptidase-4 inhibitors in type 2 diabetes. Lancet 2006;368:1696–1705
9. Lovshin JA, Drucker DJ. Incretin-based therapies for type 2 diabetes mellitus. Nat Rev Endocrinol 2009;5:262–269
10. Gutniak M, Orskov C, Holst JJ, Ahrén B, Efendic S. Antidiabetogenic effect of glucagon-like peptide-1 (7-36)amide in normal subjects and patients with diabetes mellitus. N Engl J Med 1992;326:1316–1322
11. Dupre J, Behme MT, Hramiak IM, et al. Glucagon-like peptide I reduces postprandial glycemic excursions in IDDM. Diabetes 1995;44:626–630
12. Turton MD, O'Shea D, Gunn I, et al. A role for glucagon-like peptide-1 in the central regulation of feeding. Nature 1996;379:69–72
13. Hansotia T, Maida A, Flock G, et al. Extrapancreatic incretin receptors modulate glucose homeostasis, body weight, and energy expenditure. J Clin Invest 2007;117:143–152
14. Perry T, Lahiri DK, Sambamurti K, et al. Glucagon-like peptide-1 decreases endogenous amyloid-beta peptide (Abeta) levels and protects hippocampal neurons from death induced by Abeta and iron. J Neurosci Res 2003;72:603–612
15. During MJ, Cao L, Zuzga DS, et al. Glucagon-like peptide-1 receptor is involved in learning and neuroprotection. Nat Med 2003;9:1173–1179
16. Bertilsson G, Patrone C, Zachrisson O, et al. Peptide hormone exendin-4 stimulates subventricular zone neurogenesis in the adult rodent brain and induces recovery in an animal model of Parkinson's disease. J Neurosci Res 2008;86:326–338
17. Belsham DD, Fick LJ, Dalvi PS, et al. Ciliary neurotrophic factor recruitment of glucagon-like peptide-1 mediates neurogenesis, allowing immortalization of adult murine hypothalamic neurons. FASEB J 2009;23:4256–4265
18. Li Y, Perry T, Kindy MS, et al. GLP-1 receptor stimulation preserves primary cortical and dopaminergic neurons in cellular and rodent models of stroke and Parkinsonism. Proc Natl Acad Sci USA 2009;106:1285–1290
19. Perry T, Lahiri DK, Chen D, et al. A novel neurotrophic property of glucagon-like peptide 1: a promoter of nerve growth factor-mediated differentiation in PC12 cells. J Pharmacol Exp Ther 2002;300:958–966
20. Perry T, Holloway HW, Weerasuriya A, et al. Evidence of GLP-1-mediated neuroprotection in an animal model of pyridoxine-induced peripheral sensory neuropathy. Exp Neurol 2007;203:293–301
21. Watabe K, Fukuda T, Tanaka J, Honda H, Toyohara K, Sakai O. Spontaneously immortalized adult mouse Schwann cells secrete autocrine and paracrine growth-promoting activities. J Neurosci Res 1995;41:279–290
22. Tosaki T, Kamiya H, Yasuda Y, et al. Reduced NGF secretion by Schwann cells under the high glucose condition decreases neurite outgrowth of DRG neurons. Exp Neurol 2008;213:381–387
23. Nakamura J, Kato K, Hamada Y, et al. A protein kinase C-β–selective inhibitor ameliorates neural dysfunction in streptozotocin-induced diabetic rats. Diabetes 1999;48:2090–2095
24. Livak KJ, Schmittgen TD. Analysis of relative gene expression data using real-time quantitative PCR and the 2(-Delta Delta C(T)) Method. Methods 2001;25:402–408
25. Beiswenger KK, Calcutt NA, Mizisin AP. Epidermal nerve fiber quantification in the assessment of diabetic neuropathy. Acta Histochem 2008;110:351–362
26. Arakawa M, Mita T, Azuma K, et al. Inhibition of monocyte adhesion to endothelial cells and attenuation of atherosclerotic lesion by a glucagon-like peptide-1 receptor agonist, exendin-4. Diabetes 2010;59:1030–1037
27. Tornehave D, Kristensen P, Rømer J, Knudsen LB, Heller RS. Expression of the GLP-1 receptor in mouse, rat, and human pancreas. J Histochem Cytochem 2008;56:841–851
28. Ban K, Noyan-Ashraf MH, Hoefer J, Bolz SS, Drucker DJ, Husain M. Cardioprotective and vasodilatory actions of glucagon-like peptide 1 receptor are mediated through both glucagon-like peptide 1 receptor-dependent and -independent pathways. Circulation 2008;117:2340–2350
29. Thorens B. Expression cloning of the pancreatic beta cell receptor for the gluco-incretin hormone glucagon-like peptide 1. Proc Natl Acad Sci USA 1992;89:8641–8645
30. Montrose-Rafizadeh C, Avdonin P, Garant MJ, et al. Pancreatic glucagon-like peptide-1 receptor couples to multiple G proteins and activates mitogen-activated protein kinase pathways in Chinese hamster ovary cells. Endocrinology 1999;140:1132–1140
31. Kimura R, Okouchi M, Fujioka H, et al. Glucagon-like peptide-1 (GLP-1) protects against methylglyoxal-induced PC12 cell apoptosis through the PI3K/Akt/mTOR/GCLc/redox signaling pathway. Neuroscience 2009;162:1212–1219
32. Cabou C, Campistron G, Marsollier N, et al. Brain glucagon-like peptide-1 regulates arterial blood flow, heart rate, and insulin sensitivity. Diabetes 2008;57:2577–2587
33. Jin HY, Liu WJ, Park JH, Baek HS, Park TS. Effect of dipeptidyl peptidase-IV (DPP-IV) inhibitor (Vildagliptin) on peripheral nerves in streptozotocin-induced diabetic rats. Arch Med Res 2009;40:536–544
34. Mentlein R. Dipeptidyl-peptidase IV (CD26): role in the inactivation of regulatory peptides. Regul Pept 1999;85:9–24
35. De Meester I, Durinx C, Bal G, et al. Natural substrates of dipeptidyl peptidase IV. Adv Exp Med Biol 2000;477:67–87
36. Allen BJ, Rogers SD, Ghilardi JR, et al. Noxious cutaneous thermal stimuli induce a graded release of endogenous substance P in the spinal cord: imaging peptide action in vivo. J Neurosci 1997;17:5921–5927
37. Ji RR, Zhang X, Wiesenfeld-Hallin Z, Hökfelt T. Expression of neuropeptide Y and neuropeptide Y (Y1) receptor mRNA in rat spinal cord and dorsal root ganglia following peripheral tissue inflammation. J Neurosci 1994;14:6423–6434
38. White FA, Jung H, Miller RJ. Chemokines and the pathophysiology of neuropathic pain. Proc Natl Acad Sci USA 2007;104:20151–20158